Use of Biogenic Gas Production as a Pre-Treatment to Improve the Efficiency of Dynamic Compaction in Saturated Silty Sand.

By

Devajani Borah

A Dissertation Presented in Partial Fulfillment of the
Requirements for the Degree
Master of Science

Approved July 2018 by the
Graduate Supervisory Committee:

Leon A. van Paassen, Chair
Edward Kavazanjian, Member
Claudia E. Zapata, Member

ARIZONA STATE UNIVERSITY

August 2018

ABSTRACT

One of the most economical and viable methods of soil improvement is dynamic compaction. It is a simple process that uses the potential energy of a weight (8 tonne to 36 tonne) dropped from a height of about 1 m to 30 m, depending on the project requirement, on to the soil to be compacted hence densifying it. However, dynamic compaction can only be applied on soil deposits where the degree of saturation is low and the permeability of the soil mass is high to allow for good drainage. Using dynamic compaction on saturated soil is unsuitable because upon application of the energy, a part of the energy is transferred to the pore water. The technique also does not work very well on soils having a large content of fines because of the absence of good drainage. The current research aims to develop a new technology using biogenic gas production to desaturate saturated soils and extend the use of dynamic compaction as a ground improvement technique to saturated soils with higher fines content. To evaluate the feasibility of this technology an experimental program has been performed. Soil columns with varying soil types have been saturated with substrate solution, resulting in the formation of nitrogen gas and the change in soils volume and saturation have been recorded. Cyclic triaxial tests have been performed to evaluate the change in volume and saturation under elevated pressure conditions and evaluate the response of the desaturated soil specimens to dynamic loading. The experimental results showed that soil specimens treated with MIDP under low confinement conditions undergo substantial volume expansion. The amount of expansion is seen to be a factor of their pore size, which is directly related to their grain size. The smaller the grain size, smaller is the pore size and

hence greater the volume expansion. Under higher confining pressure conditions, the expansion during gas formation is suppressed. However, no conclusive result about the effect of the desaturation of the soil using biogenic gas on its compactibility could be obtained from the cyclic triaxial tests.

DEDICATION

To my mother, Monimala Borah for her constant support and for inspiring me to be my best in whatever I do.

To my father, Dr. Indreswar Borah, who believed in me even at times when I'd lose faith in myself and told me to keep moving forward no matter what obstacles I faced.

To my sister, Rituparna Borah, who has always been my closest confidant and without whom my world would have been very dull.

To the women in STEM, my seniors and my contemporaries, whose work and stories have always inspired me to dedicate myself to my work and who are relentlessly working for a better, brighter and glass ceiling devoid world.

ACKNOWLEDGMENTS

I would like to extend special thanks to Dr. Leon van Paassen who gave me the opportunity to work with him on this project. He acted not only as my professor and mentor on the project, but also as a teammate and a friend.

I would also like to thank my two other committee members, Dr. Edward Kavazanjian and Dr. Claudia Zapata for their constant support on the project from time and again, which helped me immensely in the completion and presentation of my project.

I would also like to take this opportunity to thank Peter Goguen and Jeffrey Long, the lab managers for Geotechnical Engineering laboratories at Arizona State University for their constant support with all my lab tests.

My heartfelt thanks to all the members of the Engineering Research Center, Center for Bio-mediated and Bio-inspired Geotechnics (CBBG), especially, Liya Wang, Dr. Nariman Mahabadi, Daehyun Kim, Caitlyn Hall, for their help and support, academically or otherwise during the period of my project.

My sincere thanks to all the authors of the publications, whose works I have referenced in this thesis.

Lastly, I would like to thank the National Science Foundation Geomechanics and Geosystems Engineering and Engineering Research Center programs under grant number ERC-1449501 for their support of this project. Any opinions, findings and conclusions or recommendations expressed in this material are those of the author and do not necessarily reflect those of the NSF.

TABLE OF CONTENTS

CHAPTER Page

List of Figures

Figure Page

Figure Page

List of Tables

Table Page

CHAPTER 1

INTRODUCTION

Compaction of soils is applied in order to increase bearing capacity or liquefaction resistance or reduce residual settlement after construction. Dynamic compaction is one of the most cost-effective ground improvement methods to increase the density of soils at depth. However, its applicability is limited to granular materials like sands above ground. Impervious soils with a significant amount of fines and high degree of saturation are usually difficult to compact (Karol, 2003), as a significant amount of the impact from dynamic compaction is transferred to the water phase. Consequently, in soils with fines the elevated pore pressures cannot dissipate fast enough due to the low permeability. Several methods exist to enhance the ability to compact soils in this category, such as the placement of drains to shorten the water dissipation. Soils of this nature are to be found in bay areas, areas where the land is below ground water table, and in those areas where hydraulic fills are placed to extend land artificially into a larger water body. In the past, efforts have been made to dynamically compact soil with high fines content (Asaka,2015 ;Karunawardena and Toki, 2014) but in those cases the soil was not fully saturated. In Asaka's (2015) case study of Chiba Prefecture, Japan, it was reported that dynamic compaction of the fine grained reclaimed ground resulted in soil improvement. In this study we evaluate the potential of a newly proposed method to enhance the efficiency of dynamic compaction for saturated soils with considerable amount of fines. By stimulating biogenic gas production in situ, soils may be desaturated below the groundwater table. Presence of occluded gas in the pore space, will increase the compressibility of the pore fluid and

consequently enhance the compactibility of the soil.

Figures 1 illustrates the hypothesized path which leads to improved compaction. . Considering the soil is initially saturated, it is on the wet side of the optimum moisture content. Through biogenic gas formation the soil is desaturated (path AB). At the point optimum moisture content, the maximum density can be obtained corresponding to the compactive effort provided (path AC).

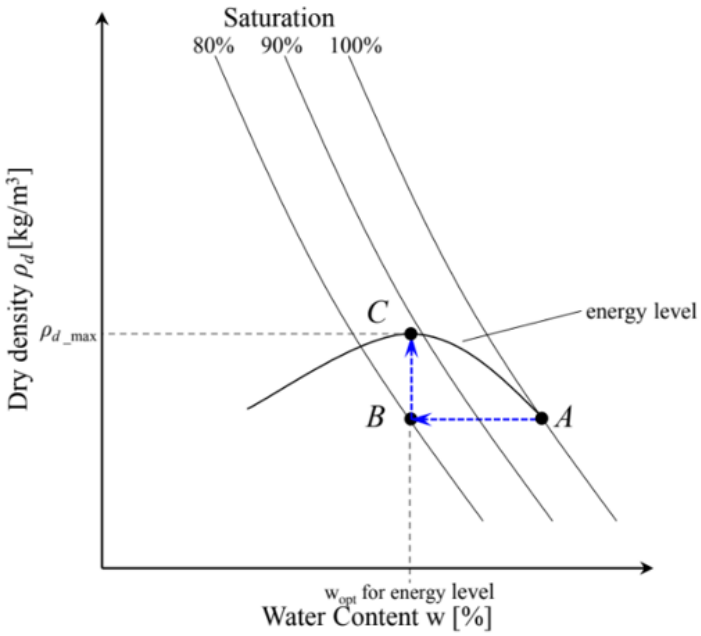

Figure 1: The proposed route of desaturation. AB – Route of desaturation. BC- Route of density increase due to compaction. (Andrag, 2017)

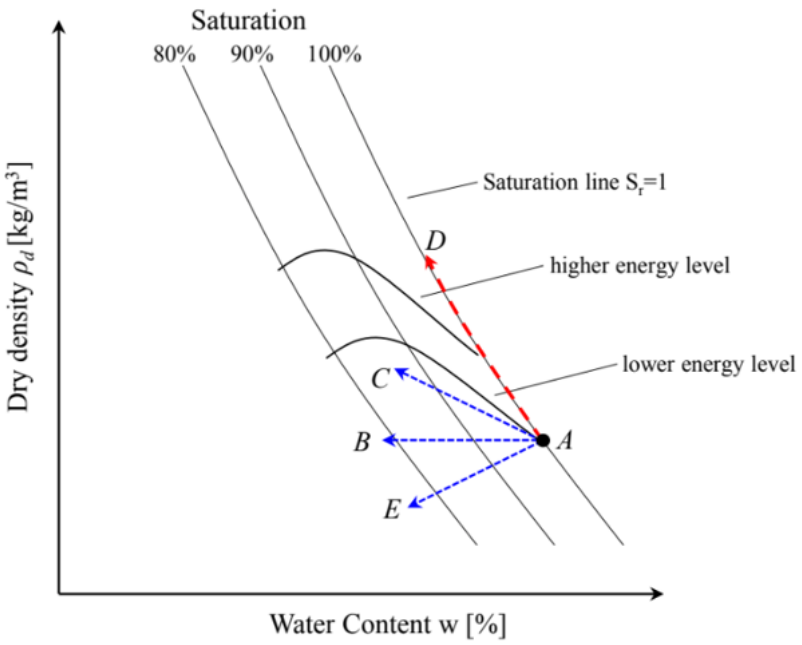

Figure 2:AC - Path of consolidation with a decrease in void ratio;AB - Path of consolidation with constant void ratio and AE- Path of consolidation with an increase in void ratio. (Andrag, 2017)

However, as shown in Figure 2, the void ratio may not be constant during desaturation through biogenic gas formation. Density may increase (path AC) or decrease (path AE). In this study, biogenic gas production induced by microbial denitrification is used as the method to partially desaturate the soil. Pham et al. (2017) confirmed desaturation of a saturated soil sample using microbial denitrification in an engineered substrate solution to be 80%. Studies on this method of desaturation has been carried out by He et al., 2013, He and Chu, 2014, He et al., 2014, and He et al., 2016, in potentially liquefiable sand by using a cultivation of denitrifying bacteria (Giovanni, 2017). In all of these studies, the focus was on liquefaction mitigation using microbially induced partial desaturation. Andrag G.M.(2017) had a similar scope, but provided inconclusive results on the compaction of silty sands through biogenic gas desaturation pretreatment. The current study uses recommendations from this previous study to see how desaturation

using biogenic gas production will impact dynamic compaction on it. One of the main concerns in his study, was that he used static loading to evaluate the compactability of desaturated soil. In this study dynamic compaction has been induced by cyclic triaxial laboratory testing, after the sample was desaturated through denitrification.

1.1 Objectives

The scope of this study is to evaluate the potential of using biogenic gas desaturation as a pretreatment on a saturated silty sand to improve the efficiency of dynamic compaction. An experimental approach was adopted to address this scope. The experiments were designed and performed with the following objectives:

1. To study the changes in the degree of saturation as a result of biogenic gas production.
2. Investigate the change in void ratio (or density) during the desaturation process under varying pressure conditions and different soil types.
3. To study the effect of biogenic gas production on the compactibility of the soil.

CHAPTER 2

LITERATURE REVIEW

2.1 Dynamic Compaction

Dynamic compaction is one of the simpler and more economically viable ground improvement techniques which requires a short treatment time (Moore et al 2007, Feng et al, 2010; Yogendrakumar and Wedge, 2014; Torrijo et al, 2016; Torrijo et al, 2017). The use of dynamic compaction is not a new technique but an improvement of an old technique used in ancient China and the Roman Empire (Torrijo et al, 2017). The technique as we know it today was first developed by Ménard and Broise in 1975. The objective of using dynamic compaction as a soil improvement technique is to improve the bearing capacity of a compressible soil applying dynamic force generated by a falling tamper (Lukas, 1992; Chow et al, 1992, Poran et al. 1992; Chow et at, 1994; Lukar, 1995; Lee and Gu 2004; Bo et al, 2009; Rollins and Kim 2010; Zekkos and Flanagan 2011; Torrijo et al, 2017). The energy applied duringdynamic compaction is about 2000 kN/m^2, reaching this value with each impact. The drop weight is about 100 to 400 kN and the drop height ranges from 10 to 20 m.

The dynamic compaction process generates compression waves and Rayleigh waves, which are transmitted through the ground and increase the packing density of the soil particles (Torrijo, 2017). Improvement of the packing of the grains in granular soil above groundwater table results in lower void volumes and increased relative density, which increases shear strength and bearing capacity and reduces residual settlement; thus improving the soil behavior (Mayne 1988; Lee and Gu 2004; Slocombe, 2004, Torrijo,

2017). In saturated granular soils however, a part of the energy is transferred to the pore water thus reducing the efficiency of the technique and increasing the chances of liquefaction due to shear failure of the soil. Which is why the current project explores the potential of using biogenic gas generation to desaturate saturated soil and increase the effectiveness of the dynamic compaction technique in these soils.

2.2 Cyclic Triaxial Testing

The application of dynamic loading in this current study is by using the cyclic triaxial testing machine. A cyclic triaxial test is a method of determining the liquefaction potential (or cyclic strength) of a soil in the laboratory, at high strain levels. The soil used for the test is either an intact or reconstituted saturated soil. The main difference between a triaxial test and a cyclic triaxial test is that, unlike in a triaxial test where the pneumatically applied deviator stress σ_d (Difference between the axial stress and the radial stress) is applied axially in a constant manner, in a cyclic triaxial test, the deviator stress is applied cyclically either under stress-controlled conditions or under strain-controlled conditions. The stress-controlled conditions are pneumatically controlled by hydraulic loaders, while the strain-controlled conditions are servo-hydraulically controlled by mechanical loaders.

The use of cyclic triaxial machine for the application of the dynamic compaction was because of the ease of controlling the rate of application of the dynamic energy and the amount of load applied.

2.3 Microbial Denitrification

Microbial denitrification can be defined as a biological process that involves the production of nitrogen gas by the action of denitrifying bacteria on suitable substrate matter. The microbes use nitrates to break down organic matter and produce nitrogen gas and biomass (Pham et al, 2016).

The production of nitrogen gas in this process of microbial denitrification not only acts a buffer to undrained dynamic loading as a result of compressibility of the gas bubbles produced in the process, resulting in increased cyclic stress ratio and reduction of P-wave velocity, but also enhances the undrained response of a soil (Andrag, 2017). In a 2012 study published by Rebata-Landa and Santamarina, connections have been established between this said phenomena and the Skempton B-value.

Many factors affect the production of the nitrogen gas in the denitrification process. These factors include pressure conditions, presence of oxygen, organic carbon availability, pH and temperature. Knowles (1982) described denitrification as "*the dissimilatory reduction, by essentially aerobic bacteria, of one or both of the ionic nitrogen oxides nitrogen oxides (NO_3^-, NO_2^-) to gaseous oxides (nitric oxide, NO, and nitrous oxide, (N_2O), which may themselves be further reduced into dinitrogen (N_2). The nitrogen oxides act as terminal electron acceptors in the absence of oxygen. The gaseous nitrogen species are major products of these reductive processes*". However, nitrite (NO_2^-), nitric oxide (NO) and nitrous oxide(N_2O), which are all possible products of the conversion of nitrate to nitrogen gas (N_2) are all harmful to the environment and also to the denitrifying bacteria itself (Andrag, 2017 ; van Spanning et al.,2006). Hence, to prevent the production of harmful byproducts during the conversion of nitrate to nitrogen

gas, nitrate and acetate have to react in the correct ratio (Andrag, 2017). In a study done by Pham (2016), the most efficient acetate to nitrate ratio (Ac/N) is identified as 0.8. The study noted that the residual nitrite concentration does not reduce to zero as is the case in an Ac/N experiment with ratio 1.2. The closer the reaction gets to the catabolic reaction (Ac/N of0.6), the greater the rate of gas production though at a greater residual nitrite concentration. The bacteria used in the process have not been classified for this study but in a 2012 study published by Rebata-Landa and Santamarina, the bacteria, *Paraccocus denitrificans* was used.

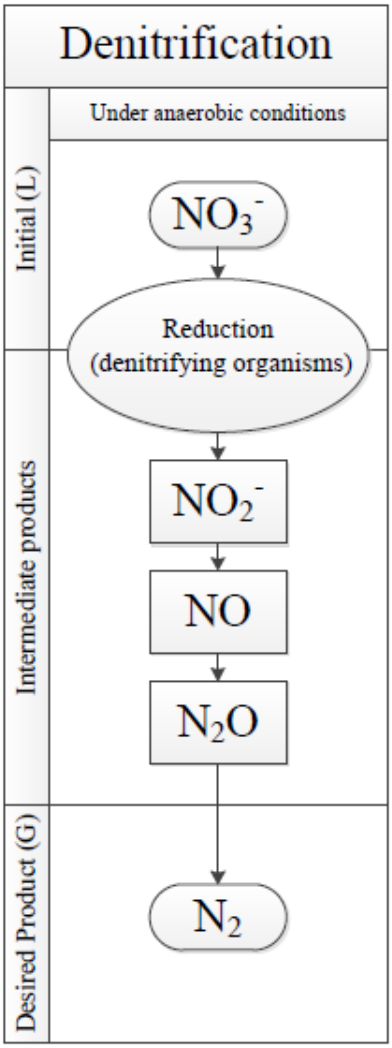

Figure 3: The process of denitrification (van Spanning et al., 2006)

The metabolic process of denitrification can be divided into anabolic and catabolic reaction: The anabolic reaction is the reaction by which bacteria synthesize biomass. (Andrag, 2017). The chemical reaction can be written as:

$$0.765C_2H_3O_2^- + 0.2NO_3^- + 0.475H^+ \rightarrow 0.45HCO_3^- + CH_{1.8}O_{0.6}N_{0.2} + 0.8H_2O$$

The catabolic reaction is a reaction, which generates energy, which can be used by the micro-organisms to grow and produce new biomass or maintain themselves (Andrag, 2017).The chemical reaction can be written as:

$$C_2H_30_2 + 1.6\ NO_3^- + 0.6H^+ \rightarrow 2HCO_3^- + 0.8N_2 + 0.8H_2O$$

The metabolic reaction is a combination of catabolic and anabolic reactions. The stoichiometry of the metabolic reaction depends on the growth rate of the micro-organisms and can be derived from the energy balance, e.g. according to Heijnen et al (1992). At maximum growth the metabolic reaction can be written as: (Pham et al, 2016)$1.18C_2H_3O_2^-(aq) + 0.93NO_3^-(aq) + 0.75H^+(aq) \rightarrow 1.37HCO_3^-(aq) + 0.37\ N_2(g) + CH_{1.8}O_{0.6}N_{0.2}(s) + 0.57H_2O(aq)$

When the substrates acetate and nitrate are supplied as calcium salts,theproduced inorganic carbon will result in the precipitation of calcium carbonate due to the presence of calcium ions. This calcium carbonate may act as cement between soil particles. It is the production of the gas (nitrogen),which is used in the MIDP. The production of calcite by this process is very minimal and slow.

Figure 4 illustrates a reaction rate model of MIDP prepared by using AQUASIM.

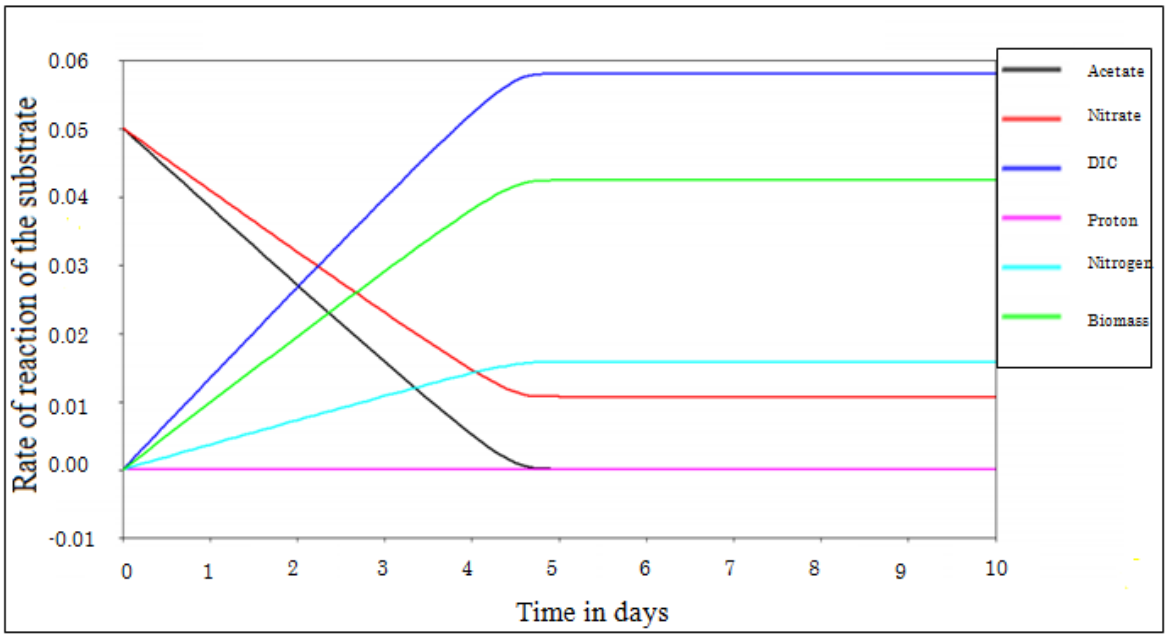

Figure 4: Concentration vs. time graph of the metabolic reaction involved in MIDP.

From Figure 4 it is clear that as the concentration of acetate is decreasing there is a decrease in the concentration of nitrates to the point of depletion around day 3.There is however an increase in the concentration of nitrogen and dissolved inorganic carbon. The amount of biomass increases but the proton concentration seems to remain the same.

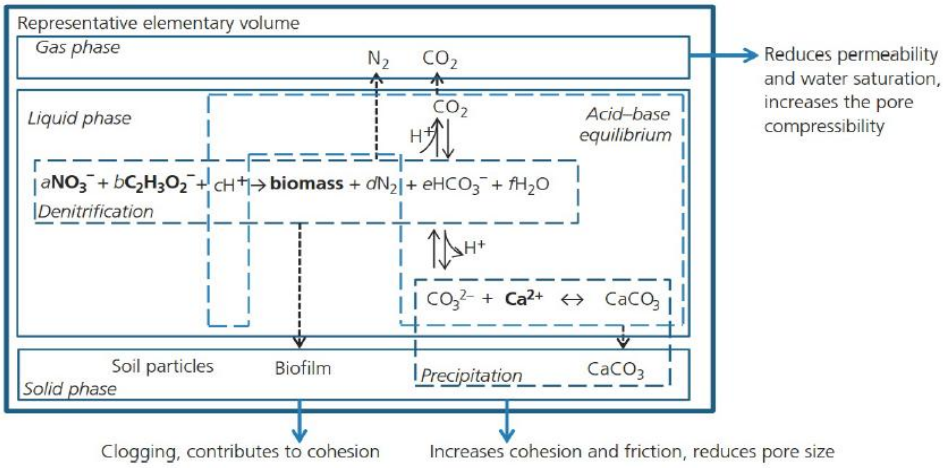

Figure 5: The process of Microbially Induced Desaturation and Precipitation (MIDP) (Pham et,al 2016)

2.4 Mechanical Effect of the Biogenic Gas on Soil Structure

Rebata-Landa and Santamarina (2012) showed that biogenic gas generation effectively reduces bulk stiffness of the pore fluid, Skempton's B Parameter relative to the soil shear stiffness, the susceptibility to liquefaction and P-wave velocity. In their study the proof of the nitrogen gas being produced biogenically can be derived from the fact that despite having no response in a soil sample treated with inoculum in any sterile conditions, there was a constant change in the P-wave velocity and gas volume. This could only be attributed to the fact that the generated gas is biomediated, since the gas generation cannot be explained by the chemical effects associated with the addition of nutrients to the soil.

When looking at the potential of using biogenic gas production as a preventive measure for the problems like liquefaction arising due to dynamic loading, Rebata-Landa and Santamarina hypothesized that the method of biogenic gas production may be more effective because biogenic gas forms submicron size bubbles which are dispersed throughout the soil mass and not just concentrated along the percolation paths as in the case of injections. However, this hypothesis needs further evaluation.

The effect of soil grain size on the early evolution of bio-mediated gas generation is significant. The soil grain size affects nucleation and entrapment of gas bubbles. It was found that fines content is directly proportional to the rate at which a stable P-wave velocity maybe reached. The higher the fines content, the faster the rate at which a stable P-wave velocity may be reached and vice-versa. Therefore, in soils with higher fines content, the rate of the P-wave reaching a stable velocity is higher than in cleaner sand.

Other factors that affect and facilitate the bubble formation of a biogenic gas are

the selection of the bacteria and nutrients. The right choice of the bacteria and the nutrients makes sure that the eventual gas produced is environmentally safe, have low solubility, facilitate good bubble formation and also experience longer residency time. However, it was recognized in the study that though nitrogen gas has all the aforementioned desirable properties, there is a possibility of producing undesirable by-products in an incomplete denitrification pathway which is environmentally detrimental and hence further analysis should go into this process.

2.4.1 Buoyancy of a biogenic gas bubble in the soil matrix

Buoyancy is the property of a material by virtue of which the body exerts an upward force, called the buoyant force, when submerged in fluids. It is expressed by the formula,

$$F_b = \rho g V$$

Where F_b = Buoyant force

ρ = Density of the fluid in which the body is submerged

g = Acceleration due to gravity

V = Volume of the body submerged

In case of gas bubbles in the pore fluid of a soil matrix, the bubbles exert a buoyant force on the surrounding media, the value of which can be calculated using the following formula,

$$F_b = (\rho_{fluid} - \rho_{gas}) g V$$

Where,

F_b = Buoyant force

ρ_{fluid}= Density of the pore fluid

ρ_{gas} = Density of the gas

g = Acceleration due to gravity

V = Volume of the body submerged

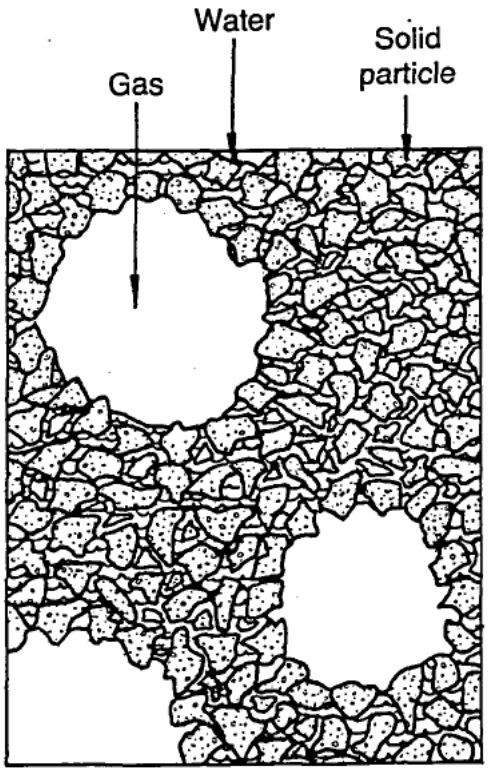

Figure 6: Gas bubble in fine grained soil (Wheeler, 1990)

Now the volume of the gas phase can be calculated using the ideal gas law formula,

$$pV=nRT$$

Where,

p is the gas pressure in atm

V = Volume of the gas

n = No. Of moles of the gas

R = 0.0821 L-atm/mole-K

T = Temperature at which the gas exists.

Here it can be hypothesized that the buoyant force is equal to the effective stress of the soil under the assumption that the effective stress of the soil is uniform throughout the soil matrix.

Since the presence of the gas, makes the soil unsaturated, for a continuum,

$$\sigma'=(\sigma-u_a)-(\sigma^s)$$

(Lu and Likos, 2006)

Where,

σ' = Effective stress

σ = Total stress

u_a = Pore air pressure

σ^s = Suction stress

$u_a-u_w \leq 0$, $\sigma^s = -(u_a-u_w)$

When,

$u_a-u_w \geq 0$, $\sigma^s = f(u_a-u_w)$

Where, f is a scaling function, which describes a link between the suction stress and matric suction.

From this entire hypothesis, (with the assumption that the effective stress is uniform throughout the entire soil matrix), it can be concluded that,

A gas bubble will disturb the existing soil condition by breaking through the pore throat when R > Pore throat size

Where, R = radius of the gas bubble

$$F_b > \sigma'$$

And the buoyant force is greater than the effective stress.

Wheeler (1990) studied the dispersion of discrete gas bubbles in fine grained soil assuming a continuum model. According to this study, the force available to resist upward motion of a large gas bubble is dependent on the undrained shear strength s_{un} of the saturated matrix. Considering the buoyancy force of the bubble F_b as P1, the resisting force P_2 can be calculated as the force required to move a smooth spherical body (the gas bubble) within an infinite volume of soil with strength s_{un}. The saturated matrix is assumed to be a rigid, perfectly plastic material.

Thus, P_2 is given by,

$P_2=10*\pi*a^2*s_{un}$

Where, a = radius of the bubble

s_{un}= Undrained shear strength of the soil.

Since $P_1 = P_2$,

The critical bubble radius, a_c is given by,

$a_c=(7.5*s_{un})/ (\gamma_m-\gamma_g)$

where,

a_c– Critical bubble radius

γ_m – Unit weight of saturated soil matrix

γ_g– Unit weight of gas

s_{un}–Undrained shear strength of the soil matrix

From this equation, we learn that the critical radius of the gas is directly proportional to the undrained shear strength of the saturated soil matrix and varies

inversely with the unit weight of the soil. A bubble with a radius greater than the critical radius will rise through the sediment due to sufficient buoyancy, while a bubble with radius smaller than or equal to will stay in its original position. The speed at which the bubble rises will depend on the viscous effects of the pore fluid. (Wheeler, 1990)

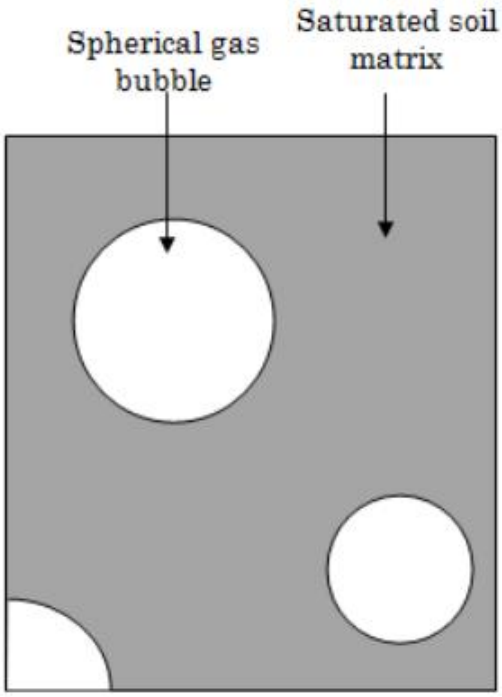

Figure 7: The continuum model (Wheeler, 1990)

2.5 Relation between soil grain size, soil pore size and gas migration

It is important to correlate the soil grain size with the soil pore size because that will enable us to explain the behavior of the soil structure once the production of biogenic gas occurs. A gas bubble will disturb the existing soil condition by breaking through the pore throat when

R> Pore throat size

Where, R = radius of the gas bubble

According to a study done by Arya and Paris in 1981, the mean pore radius (r_m) is directly proportional to the mean particle radius (r) assuming cubic close packed assemblage of uniform sized particle. That would mean that the larger the grain size, larger is the particle size and vice versa. This can explain that with smaller pore sizes the generated gas bubble will be unable to escape the soil structure and hence result in the swelling (volume expansion) of the soil under low confinement conditions.

Another factor that has to be taken into account while studying the migration of the gas bubble is the air entry value. Air entry value can be described as the matric suction from which air starts to penetrate into the soil that is also called bubbling pressure (Corey, 1977). Matric suction (s) can be defined as the difference between the gas pressure (u_a) and the pore water pressure (u_w). Air entry value can be derived from the soil water retention curve. The soil water retention curve is the relation between the matric suction of a soil and its volumetric water content (θ). The air entry value derived from a soil water retention curve is inversely proportional to the particle size. The smaller the grain size, higher the air entry value and vice versa. Gas bubbles can only migrate in a soil structure when the air entry value is exceeded. Soil water retention curves have been obtained using the HYPROP ® device.

CHAPTER 3

MATERIALS AND METHODOLOGY

In order to evaluate the potential of MIDP to improve the efficiency of dynamic compaction, various experiments were performed using different soil types. This chapter describes materials andtest procedures used throughout the study.

3.1 Soil types and soil characteristics

Three soils were used in this study. A locally available soil containing significant fraction of fines was collected from a stockpile at East Guadalupe Road in Tempe, Arizona. For the remainder of this document this soil type is referred to as ASU soil. This soil was usedin most of the experiments. For comparison two other soils, Ottawa F-60 and Ottawa 20-30 were used. Their properties have been derived from existing literature. The soils were classified according to ASTM D2487- 06 (ASTM, 2006). Grain size distribution was determined according to ASTM C136 (ASTM, 2014). In case the soil contained fines a wet sieving method was employed. The Atterberg limit tests were performed in accordance to ASTM D4318 - 17e1 (ASTM, 2017)to determine the plastic limit, liquid limit and plasticity index of the fines fraction of the soil.

3.2 Standard Proctor Test

A standard proctor test was carried out in accordance with ASTM - D698-07 (ASTM, 2007) to find the maximum dry density and the optimum moisture content of the ASU soil. A mould of height 116.83 mm (11.683 cm or 4.59 inches) and diameter 101.02 mm (10.102 cm or 3.97 inches) and volume 109399002.7mm^3 (10939.9 cm^3 or 3260.79

inches^3) was used for this test. The initial water content of the soil was 1.5%. The soil was placed in three layers in the mould and a 5.5 lb hammer was used to tamp the soil layer with 25 blows to each layer. The drop height of the hammer is 12 inch and the energy transferred is 12,400 ftlb/ft^3. The weight of the soil was measured post the tamping and it was recorded. A small plug of soil was collected from the middle of the compacted sample and used for water content measurement. A total of 3 kg of soil was used for the standard proctor test. The wet density (γ) of the soil is measured by -

$$\gamma = \frac{m_T}{V_T}$$

Where,

m_T – Weight of the compacted soil

V_T – Volume of the mould

From this the dry density can be measured as,

$$\gamma_d = \frac{\gamma}{1 + w}$$

Where w is the water content.

While plotting this graph the air voids curve is also plotted on the same graph. Air voids curve is the line showing the saturation of the soil specimen. The maximum dry density is never higher than the zero air voids curve or the curve corresponding to 100% saturation. The saturation curve is plotted using the following formula,

$$\gamma_d = \frac{G_s * \gamma_w}{1 + \frac{w.G_s}{S}}$$

Here,

γ_d– Dry density of the soil

G_s – Specific gravity of the soil

γ_w– Unit weight of water

w – Water content of the soil

S – Saturation

By plotting the $\gamma_d$value vs the w value, the air voids curve/saturation curve is obtained.

3.3 Soil Water Retention Curves (SWRC)

The soil water retention curves for the soils samples were determined using the HYPROP method (UMS, 2016).

3.4 Preparation of substrate solutions and enrichment of denitrifying bacteria

For the current test, a wet soil along the bank of Tempe Town Lake was sampled and used as the source from which the denitrifying bacteria were enriched. A substrate solution was prepared containing 25 mmol/l (or 5.9 g/l) of Calcium Nitrate ($Ca(NO_3)_2$and 25 mmol/l (or 4.4 g/l) of Calcium Acetate $Ca(C_2H_3O_2)_2$. Nutrients were added to stimulate enable microbial growth, which included

0.012 g/l Ammonium Chloride (NH_4Cl),

0.01 g/l of Iron(ii) Sulphate Heptahydrate ($FeO_4S \cdot 7H_2O$),

0.01 g/l of Calcium Chloride ($CaCl_2$),

0.75 g/l Potassium Dihydrogen Phosphate (KH_2PO_4),

2.5 g/l Dipotassium Phosphate (K_2HPO_4)and 1 ml/l trace element solution. The trace element solution (SL12B) contained

3 g/l Disodium Ethylenediaminetetraacetate Dihydrate(Na_2-EDTA.$2H_2O$),

1.1 g/l Ferrous sulfate heptahydrate ($FeSO_4 \cdot 7H_2O$),

0.1Dg/l Cobalt Chloride Hexahydrate ($CoCl_2 \cdot 6H_2O$),

0.05 g/l Manganese Chloride Dihydrate ($MnCl_2 \cdot 2H_2O$),

0.042 g/l Zinc (II) Chloride ($ZnCl_2$),

24 mg/l Nickel (II) Chloride Hexahydrate ($NiCl_2 \cdot 6H_2O$),

0.18 g/l Sodium Molybdatedihydrate ($Na_2MoO_4 \cdot 2H_2O$),

0.3 g/l Boric Acid (H_3BO_3), and

2 mg/l Copper Chloride Dihydrate ($CuCl_2 \cdot 2H_2O$).

Chemicals were purchased at Sigma Aldrich. Solutions were prepared using deionized water. The substrate solution was inoculated using 20 ml bacteria culture. The solution was kept at a temperature of 23^{o}C to 26 ^{o}C.

During the incubation and enrichment of the denitrifying bacteria, pH and the electrical conductivity were measured at regular time intervals to monitor the consumption of substrates. During a seven day incubation period, the pH remained around neutral , while the electrical conductivity decreased from 10.12 mS/cm to 2.79 mS/cm.

3.5 Graduated cylinder tests to evaluate the effect of biogenic gas formation under low confinement conditions

To evaluate the effect of biogenic gas formation on the change in volume and saturation of soils, experiments were performed using graduated cylinder. Figure 8 shows a typical set-up for the graduated cylinder tests.

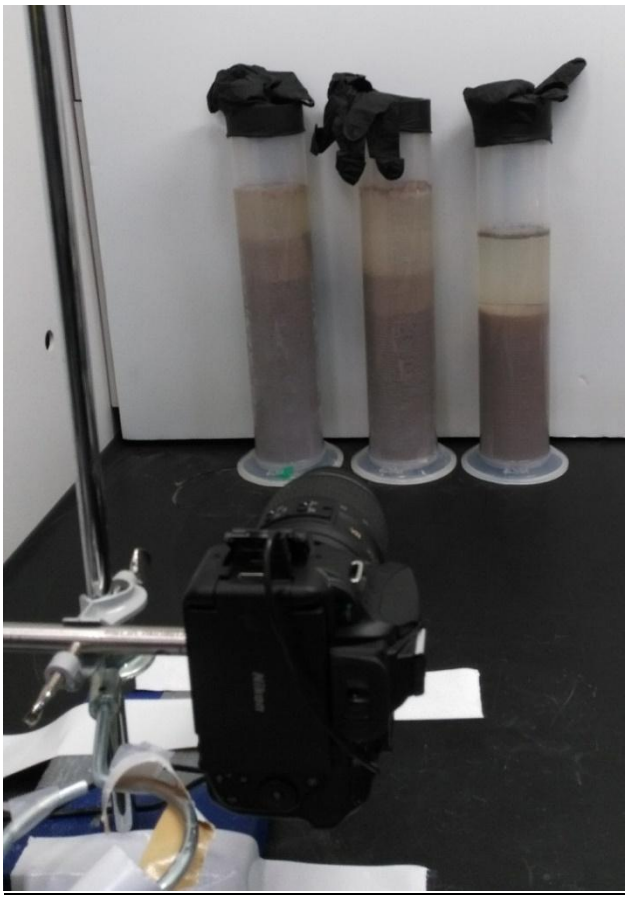

Figure 8: Typical set up for the graduated cylinder tests

Clear plastic 1 litre columns were filled with about 500 to 735 mL of inoculated substrate solution, in which a measured amount of dry soil specimen was pluviated. The columns were sealed with a rubber glove to limit evaporation and escape of gas phase. A camera was used to monitor the change in soil and liquid volume of the three columns by taking pictures at regular time intervals every 30 minutes. The initial soil conditions of the graduated cylinder tests are shown in Table 1.

Table 1 – Initial conditions of the graduated cylinder tests

		ASU Control	**ASU 1**	**ASU 2**	**ASU 3**	**O 20-30**	**OF60**
Soil type		ASU Soil	ASU Soil	ASU Soil	ASU Soil	Ottawa 20-30	F-60
Liquid	Units	Water	Substrate Solution	Substrate Solution	Substrate Solution	Substrate Solution	Substrate Solution
$\mathbf{m_d}$	[g]	650	772	642	503	760	766
$\mathbf{V_b}$	[ml]	515	635	499	500	462	475
$\mathbf{V_t}$	[ml]	790	790	800	925	865	930
$\mathbf{V_s}$	[ml]	245	291	242	190	287	289
$\mathbf{V_w}$	[ml]	525	499	558	735	578	641
$\mathbf{V_{pw}}$	[ml]	270	334	253	310	175	183
$\mathbf{V_g}$	[ml]	0	0	0	0	0	0
e	[-]	1.10	1.15	1.04	1.64	0.61	0.63

The bulk soil volume, Vb, and total volume, Vt, were interpreted from the pictures. Using an assumed specific gravity, Gs, of 2.65 the volume of solids, Vs, is calculated using:

$$Vs = \frac{m_d}{Gs}$$

Consequently the total water volume, V_w, and the pore water volume, V_{pw}, are calculated using:

$$V_w = V_t - V_s \text{ and } \; V_{pw} = V_b - V_s$$

Assuming the soil is initially fully saturated, the volume of gas, Vg, is initially considered to be zero. Considering evaporation is negligible V_w is constant. Hence, the entrapped volume of gas can be calculated using:

$$V_g = V_t - V_s - V_w$$

And the remaining volume of pore water can be calculated using:

$$V_{pw} = V_b - V_s - V_g$$

Consequently the void ratio, e, is calculated using:

$$e = \frac{V_b - V_s}{V_s}$$

And the degree of saturation, S, is calculated using:

$$S = \frac{V_{pw}}{V_g + V_{pw}}$$

3.6 Cyclic Triaxial Test

Cyclic triaxial tests were carried out on two soil specimens – one untreated and the other specimen treated with the inoculum. The cyclic triaxial test was carried out in accordance with the ASTM D-3999 and D 5311.For the current study, the STX-050 Pneumatic Soil Triaxial System by GCTS Testing Systems was used. The specimen were prepared by the method of wet pluviation to ensure complete saturation. The samples were prepared in a sealed watertight rubber membrane, which was fitted inside a split mould. A vacuum tube was attached to the mould to ensure that the rubber membrane completely fitted within it and there was no air between the membrane and the mould wall. The set up was then filled with water/inoculum to about half and soil was added slowly to it, occasionally tamping it gently to make sure that the soil is well compacted, but not consolidated. The sample in the rubber membrane was then put in a confined triaxial chamber where it was subjected to a confining pressure. An axial load of 100 kPa was applied to the top of the specimen and the samples are consolidated isotropically with equal axial and radial stress. Following the saturation and consolidation, the

specimen is made to undergo sinusoidally varying axial load. The frequency of this cyclic load was 1 Hz and it was repeated for 300 cycles. The cyclic load was determined using a Cyclic Stress Ratio(CSR) value of 0.3. CSR was first defined by Seed and Idriss in their 1971 paper. It is the ratio between the maximum cyclic shear stress (σ_{dc}) to the initial effective confining pressure (σ'_{3c})

$$CSR_{tx} = \sigma_{dc}/2\sigma'_{3c}$$ (O'Donnell, 2016).

Using this relation, since the initial effective confining pressure was 100 kPa, the cyclic load used for both the tests was 60 kPa. In both the cases the cell pressure was 207 kPa and pore pressure was 106 kPa. The main difference between the untreated and the treated specimen was that in the untreated specimen the consolidation and cyclic loading was done 24 hours after the sample was prepared ;while for the treated specimen, both the tests were done after a period of 5 days during which the sample is set standing and the denitrifying bacteria produces the nitrogen gas essentially desaturating the sample during the process.

Figure 9: The STX-050 Pneumatic Soil Triaxial System (GCTS Testing Systems)

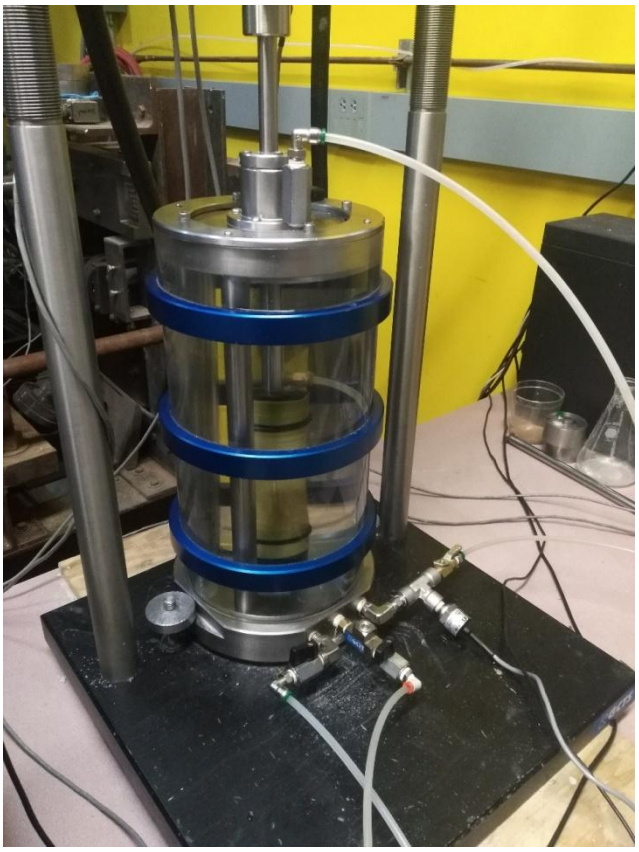

Figure 10: Typical set up for the Cyclic Triaxial Test

After the application of the cyclic load, the axial strain ε_a vs time and volumetric strain (ε_v) vs time is plotted.

Here, ε_a= ((New length – Original length)/Original length)*100

ε_v = ((New volume – Original volume)/Original volume)*100

CHAPTER 4

RESULTS AND DISCUSSIONS

4.1 Soil types and characteristics

Figure 12 shows the results of the sieve analysis of the three soils used in this study. Interpreted values of the sieve analysis, the results of the Atterberg limit tests and the resulting soil classification are shown in Table 4.

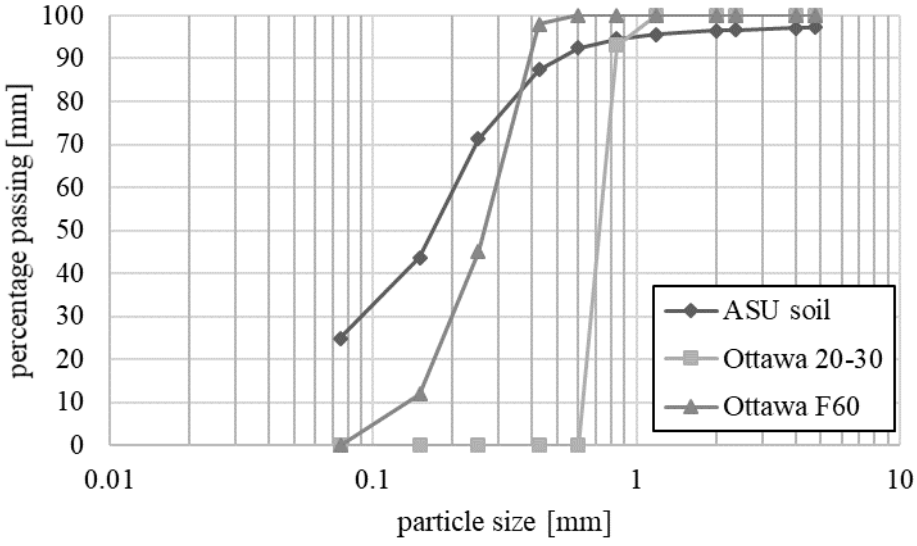

Figure 11: Sieve analysis results for the soil types used in this study

Table 3: Soil index properties and classification

Soil Name	*ASU Soil*	*Ottawa 20-30*	*F-60*
D10 (mm)	0.089	0.65	0.15
D30 (mm)	0.181	0.67	0.18
D60 (mm)	0.34	0.72	0.25
Cc	1.086	0.96	0.86
Cu	3.82	1.11	1.67
LL(%)	37	n.a.	n.a.
PL (%)	31	n.a.	n.a.
PI (%)	6	n.a.	n.a.
Soil classification (USCS)	SM	SP	SP

In which, $D_{10,}$ D_{30},D_{50} and D_{60} are the grain size diameters at which 10, 30, 50 and respectively 60 % of the grain size is passing the sieve, C_c is the Coefficient of curvature: $(D_{30})^2/(D_{10}*D_{60})$, C_u is the Coefficient of uniformity: $(D_{60})/(D_{10})$, LL is the liquid limit, PL is the plastic limit, PI is the plasticity index. Based on the results of sieve analysis and the Atterberg limit tests the ASU soil is classified as a low plasticity silty sand (SM). The Ottawa 20-30 and Ottawa F60 sands are both classified as poorly graded sand. The complete results of the classification tests have been included in the appendix.

4.2 Standard Proctor Test

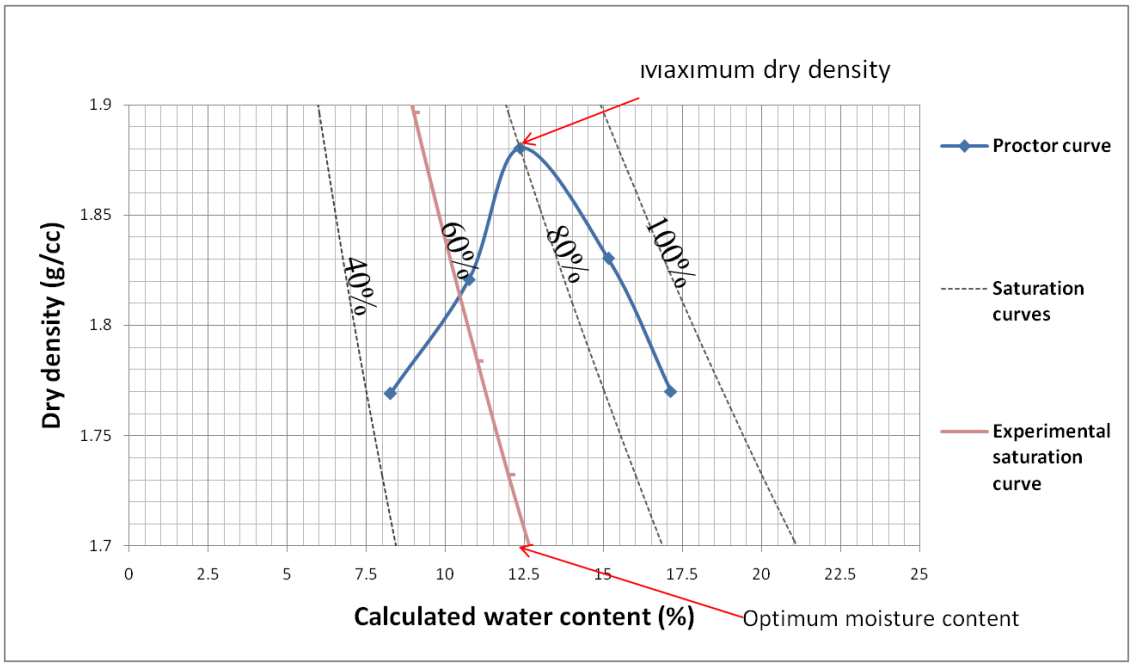

Figure 12 : Standard Proctor Curve

From Figure 12, it is visible that the maximum dry density is 1.88 g/cc for the ASU Soil with the optimum moisture content being 12.36 %. The maximum dry density is achieved at 80% saturation (or 20% air voids). The red line here depicts the experimental saturation curve. It was found that the total desaturation achieved by the biogenic gas formation is 40%, thus bringing the soil saturation, S, to 60%. This was calculated using the formula , $S = V_w / (V_w + V_g)$

Thus, S = (225.41)/(150+225.41) = 0.6

Where, V_w is the volume of pore water and V_g volume of gas formed. The maximum dry density is seen to be achieved at 80% saturation. Hence care has to be taken to make sure that the desaturation process is stopped at 80% saturation to achieve maximum density for silty sands.

4.3 Graduated Cylinder Tests

The results of the graduated cylinder tests are shown in Figure 13 to 17. Figure 13 shows the change in void ratio in time as a result of biogenic gas production. Figure 14 shows the change in saturation. Figures 15 and 16 show the initial and final images of the graduated cylinder tests, whereas Figure 13 shows the change in void ratio in time as a result of biogenic gas production and Figure 14 shows the change in saturation.

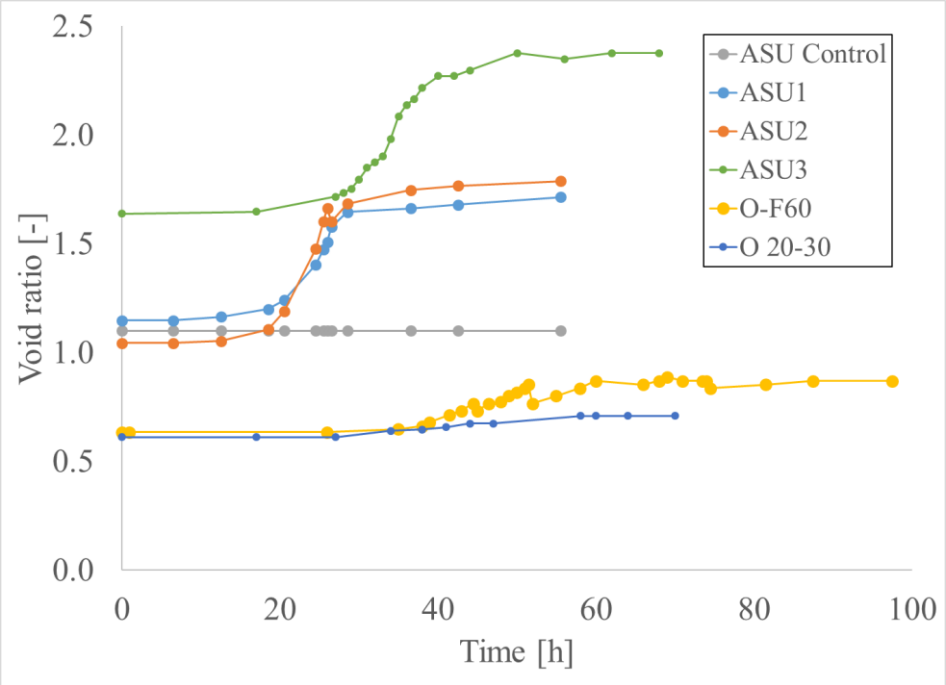

Figure13: Void ratio vs time for the graduated cylinder tests

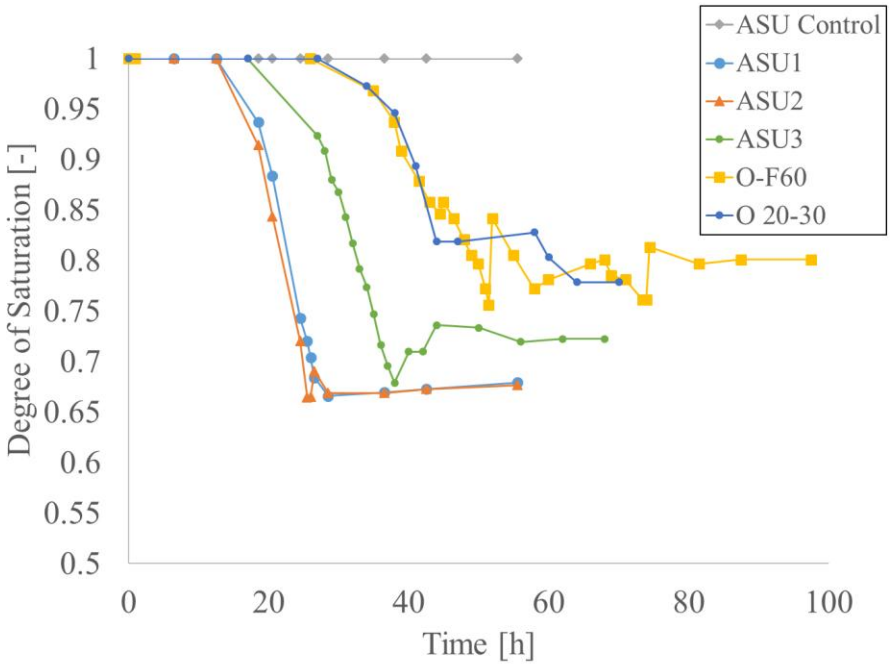

Figure14: Saturation vs time for the graduated cylinder tests

From Figure 13 it is clear that while the void ratio of the control experiment does not increase in time, while for all other soil samples, which have been pluviated in an inoculated substrate solution the void ratio increases and the degree of saturation decreases. An initial lag phase of 20-30 hours is observed in which the bacteria do not produce gas yet and the void ratio and degree of saturation remain constant. Once the bacteria start to produce gas, there is a significant increase in the void ratio and there is visible production of the gas in the form of gas lenses in the columns (Figure 16). After 20 to 50 hours the void ratio and saturation reach their maximum respectively minimum values. Over the next 40 to 50 hours still additional gas formation is being observed. However, during this stage the additional gas formation does not lead to any further increase in void ratio or decrease in saturation, but just some fluctuations as a result of trapped gas escaping from the soil columns. In some cases, particularly of the ASU soil,

some fine grained soil particles at the soil surface stick to the gas bubbles, float upward and form a foam at the water surface, making it difficult to interpret the total volume in the graduated cylinder. Once the gas production halts the void ratio and saturation are seen to be constant.

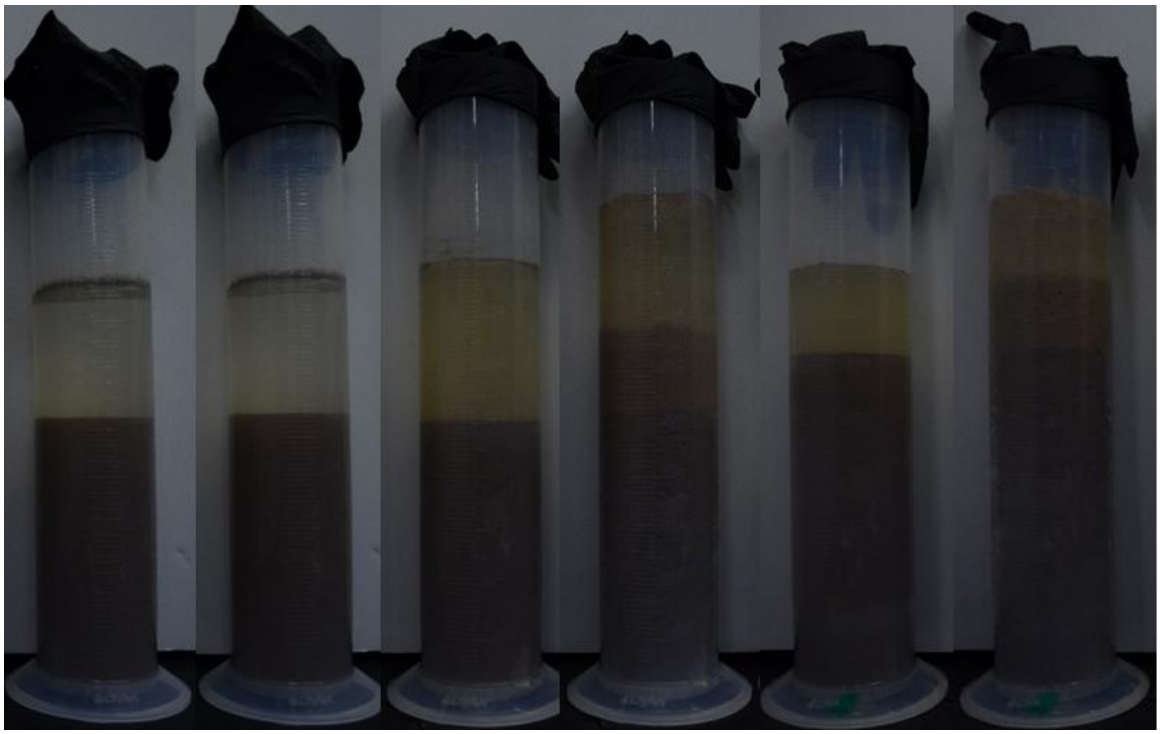

Figure 15 : Initial and final conditions of the graduated cylinder tests for ASU control (left), ASU1 (middle) and ASU2 (right).

The test results illustrate the effect of pore throat size on the gas entrapment potential. Among the three samples tested, the effective grain size, D10, of the ASU Soil is the smallest. The Ottawa 20-30 sample has the largest effective grain size. There is a direct correlation between the size of the soil effective grain size and the pore throat of the sample. Hence, the larger the effective grain size, the larger is the pore throat size and vice versa. The smaller pore throat size allows for greater entrapment of the gas hence leading to a larger increase in void ratio and larger decrease in saturation than the F-60

sand or the Ottawa 20-30 sand.

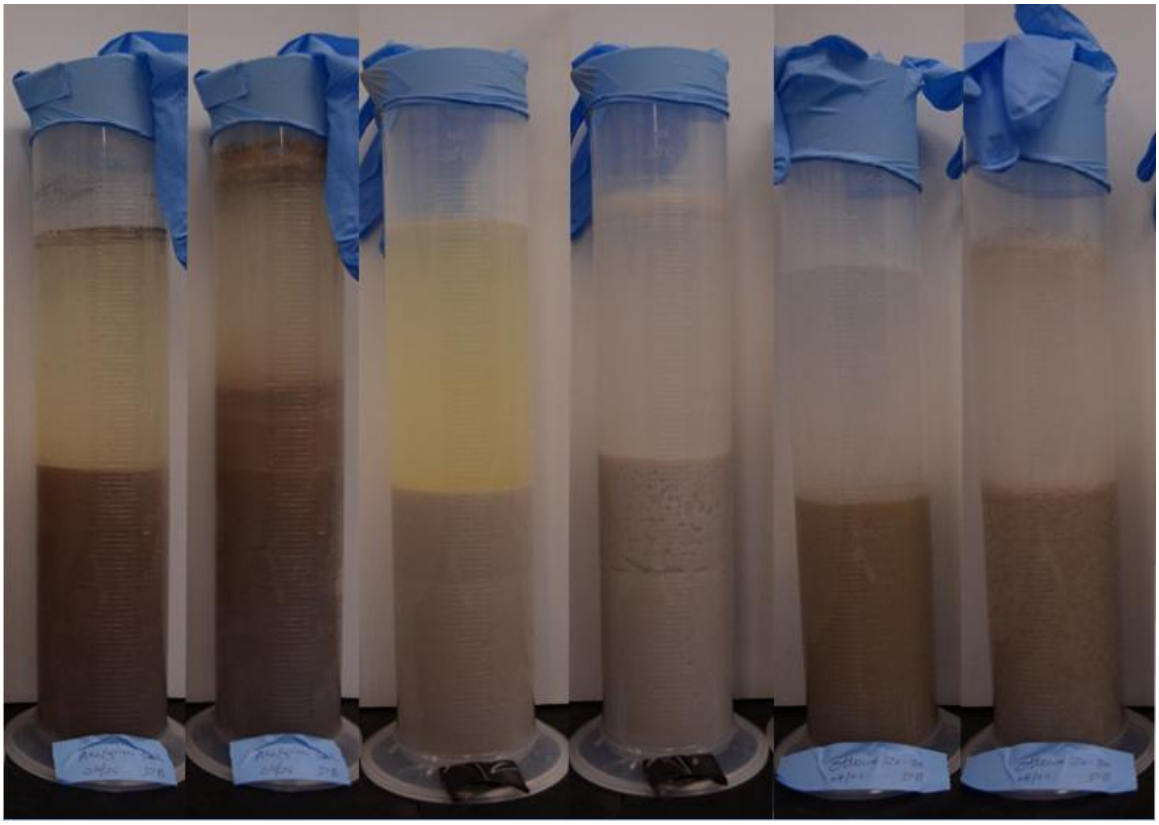

Figure 16: Initial and final conditions of the graduated cylinder tests for ASU3 (left), Ottawa F60 (middle) and Ottawa 20-30 (right) soils.

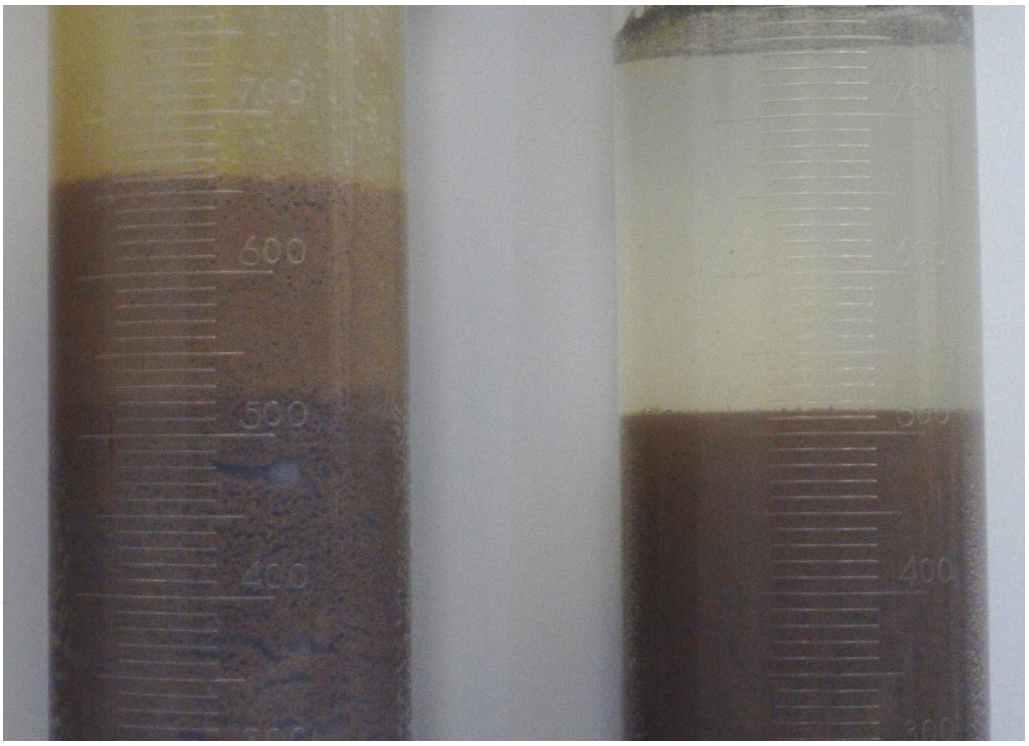

Figure 17: Gas lense formation can be seen in the treated column of ASU soil, ASU2 (left) due to the disruption of the soil matrix upon production of biogenic gas. ASU control is shown on the right

4.4 Soil Water Retention Curve (SWRC)

Figure 18 shows the results from the HYPROP test.

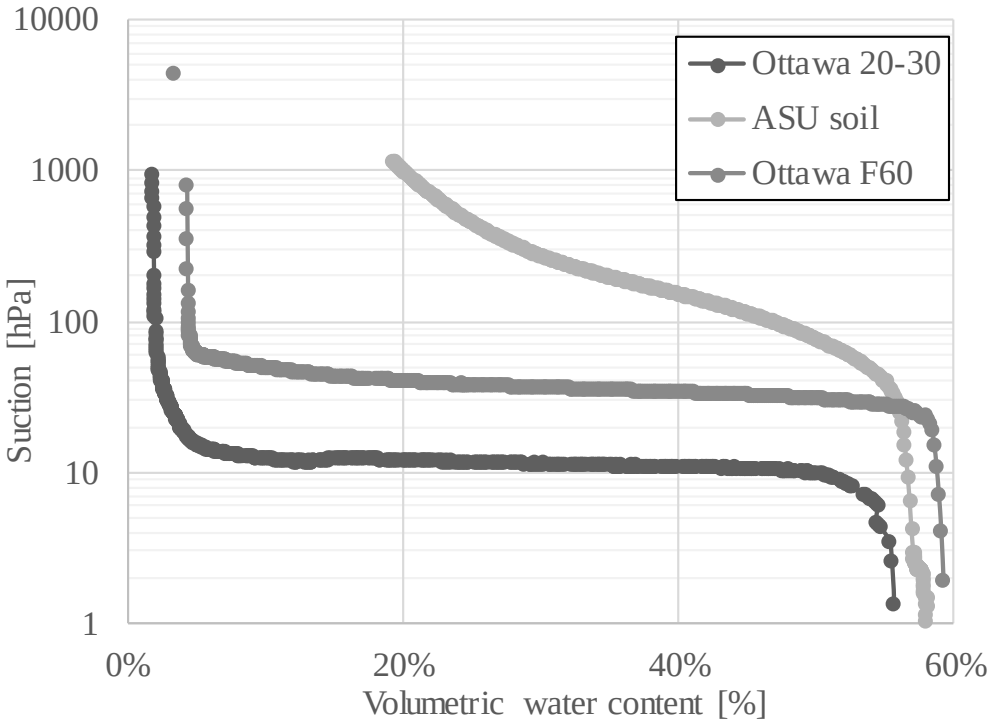

Figure 18: Soil Water Retention Curves for the different soil types.

The results for the ASU Soil (AZ soil with fines) and the F-60 soil has been experimentally observed while the results for the Ottawa 20-30 has been obtained from existing literature. It is seen that, as expected the air entry value for the ASU soil is higher than the other two soils. The Air Entry Value (AEV) is calculated from the first inflection point on the Soil Water Retention Curve. This clearly shows the correlation of the AEV and the fines content of the soil and hence the volume expansion. The ASU soil has the highest fines content in comparison to the other soils. Expectantly it also has higher AEV.

A gas bubble can only migrate upwards when the gas pressure exceeds the required capillary pressure to squeeze through the pore throats (van Paassen et al 2018, Haines 1930, Brooks and Corey 1964). This results in high volume expansion of the ASU soil because as observed by van Paassen et al (2018), during the upward migration of gas bubbles, they may get stuck below layers of low soil permeability, such as silt and clay. In such a case the gas pressure may not be able to exceed the air entry pressure of the above soil layers and as a result laterally spread to form a gas pocket as is observed with the ASU soil. The intrinsic permeability of the may also be affected by the formation of the biomass and solid minerals produced during metabolism.

4.5 Cyclic Triaxial Test

The main motives for the conduction of the cyclic triaxial test were:

1. To measure changes in saturation and void ratio during the consolidation and reaction phase and evaluate whether swelling or sample disturbance would occur during the desaturation process under higher confining pressures,
2. To determine the effect of desaturation on the compactibility of a silty sand under cyclic loading conditions.

For that purpose two tests were performed: one on treated and the other on untreated ASU soil. During the consolidation phase, a significant difference was observed for the volume change in the pressure controller, which was connected to the bottom of the sample. During the consolidation phase of the triaxial tests the samples were allowed to drain through the bottom when the effective confining pressure was applied. Figure xx shows the response in strains for the consolidation phase untreated triaxial test. After an

immediate compressive strain (about 0.2% axial, 1.3% volumetric and 0.5% radial strain), the volumetric and axial strain showed a gradual reduction, while liquid was seeping into the sample from the pressure controller.

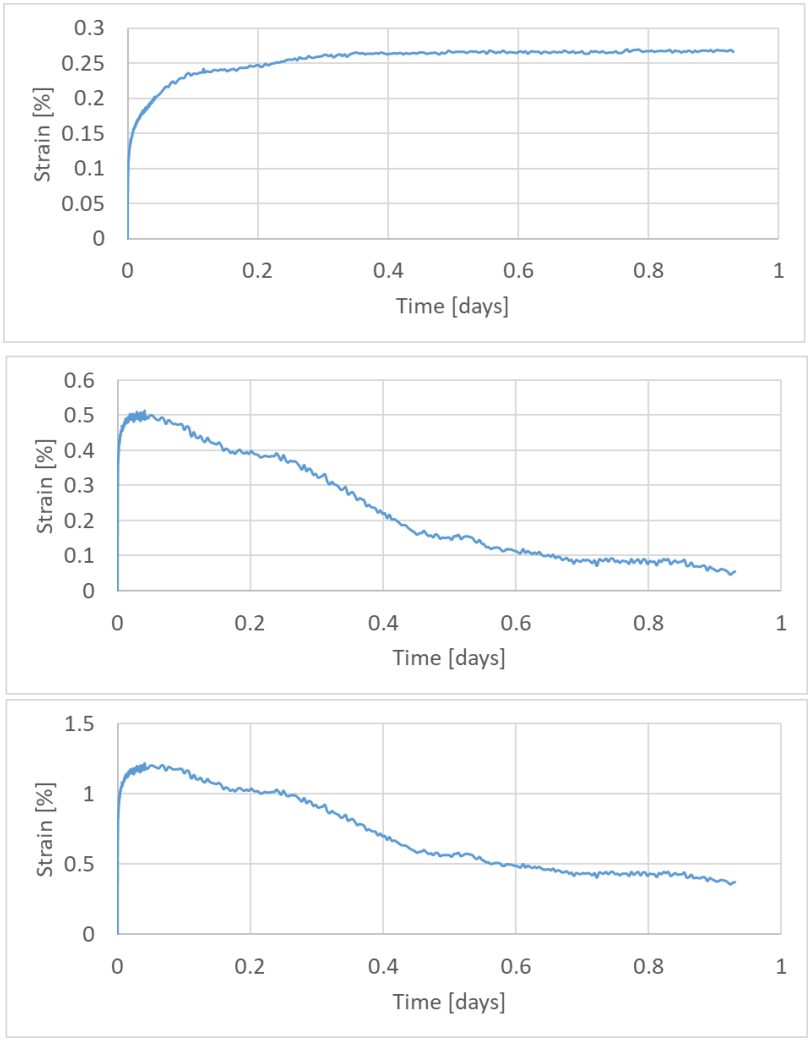

Figure 19 (a): Calculated axial (top), radial (middle) and volumetric (bottom) strains during the consolidation phase of cyclic triaxial tests for the untreated and treated sample.

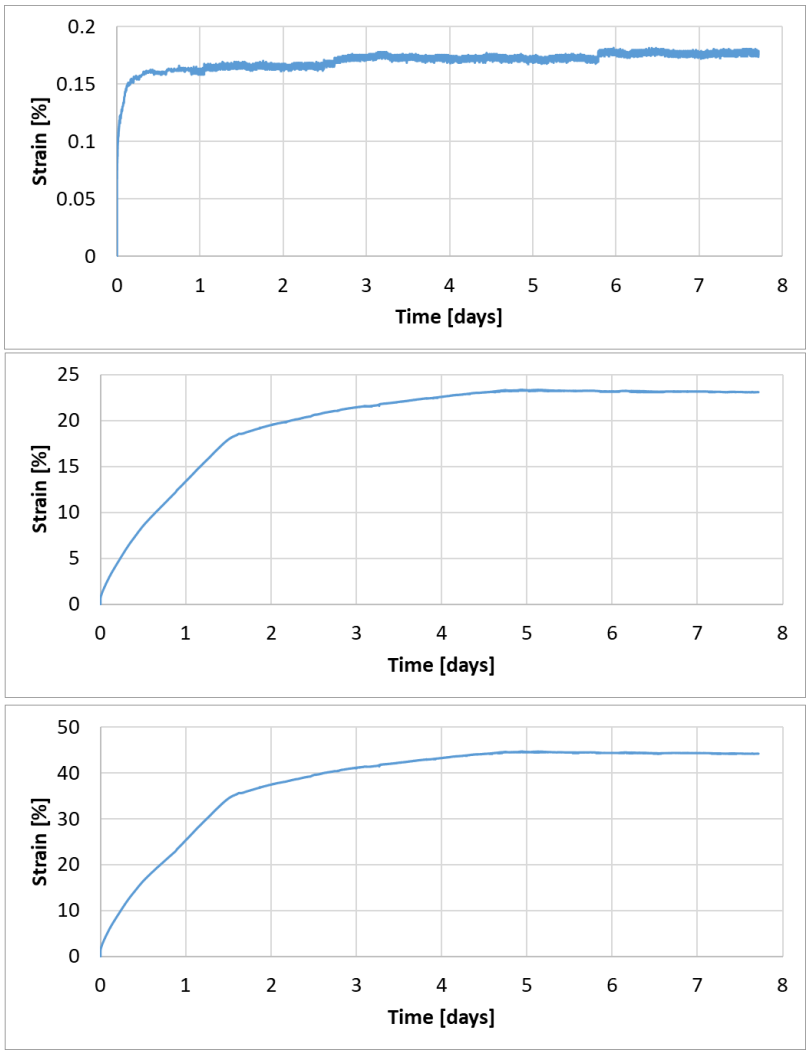

Figure 19 (b): Calculated axial (top), radial (middle) and volumetric (bottom) strains during the consolidation phase of cyclic triaxial tests for the treated sample.

Whether this decrease in volume is due to a gradual saturation of the sample or actual radial extensional deformation of the sample is unclear. The treated sample showed a similar axial strain, but the calculated radial and volumetric strains seemed to increase for a period of 4 days to reach unrealistically large values of 23 and 43%. In this case it is seems obvious that expelled liquid volume in the collected through the volume controller does not represent the volume change of the sample, but is due to the biogenic gas formation, which was confirmed visually as the sample did not show significant

shrinkage as a result of consolidation. The fact that the axial strain between of the treated sample was similar to the untreated sample confirms the hypothesis that swelling of the sample during biogenic gas formation is suppressed under conditions of sufficiently high confining pressure.

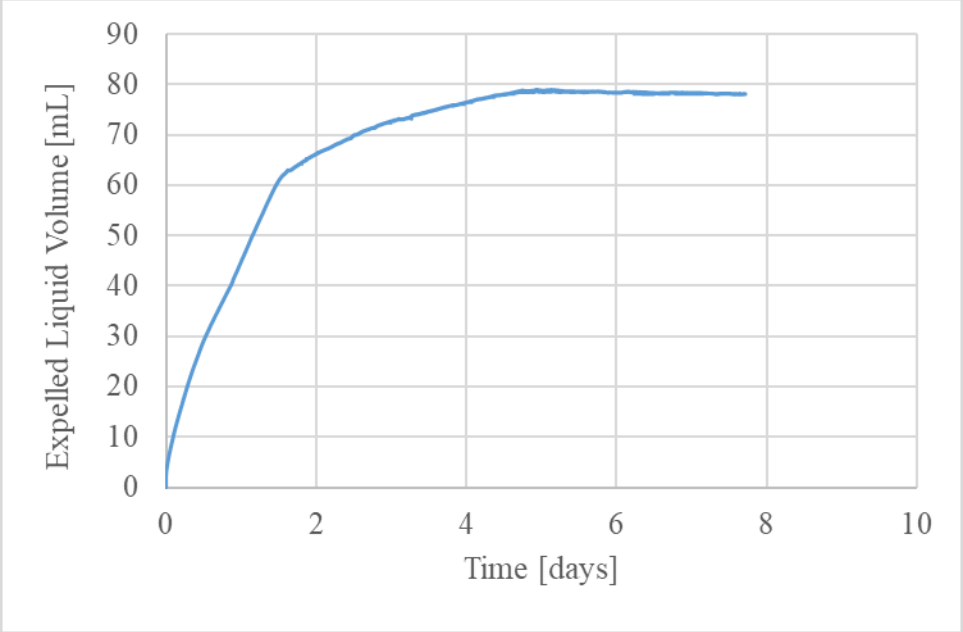

Figure 20: Expelled liquid volume during the consolidation phase of the treated sample

Figure 24 shows the expelled liquid volume during the consolidation (and reaction) phase of the treated sample. Based on concentrations of the substrate solution (50 mmol nitrate per litre) and the total pore volume of the sample (about 80 mL) and assuming all the nitrate would be converted to nitrogen gas and the gas pressure would be equal to the pore pressure (a pore pressure of 100kPa, corresponds to an absolute gas pressure of 200 kPa), the expected volume of gas was estimated at 30 mL and resulting degree of saturation would range between 40 and 50%. The volume of expelled liquid after 4 days was about 80 mL. This larger volume may be due to:

1. Some compaction of the sample: the volumetric strain during the consolidation phase is expected to be similar to the untreated sample, about 1%,
2. A larger volume of injected substrate solution: the filters and tubing may also contain substrate solution, which may double the volume of injected liquids and consequently double the amount potential amount of gas volume;
3. Some remaining substrates in the inoculum, which lead to additional gas formation
4. Formation of carbon dioxide as an additional source of gas
5. Inaccuracies in the measurements

Cyclic loading was applied in order to mimic the effect of dynamic compaction and evaluate the effect of desaturation on the compactibility of the soil. Results of the first tests are shown below.

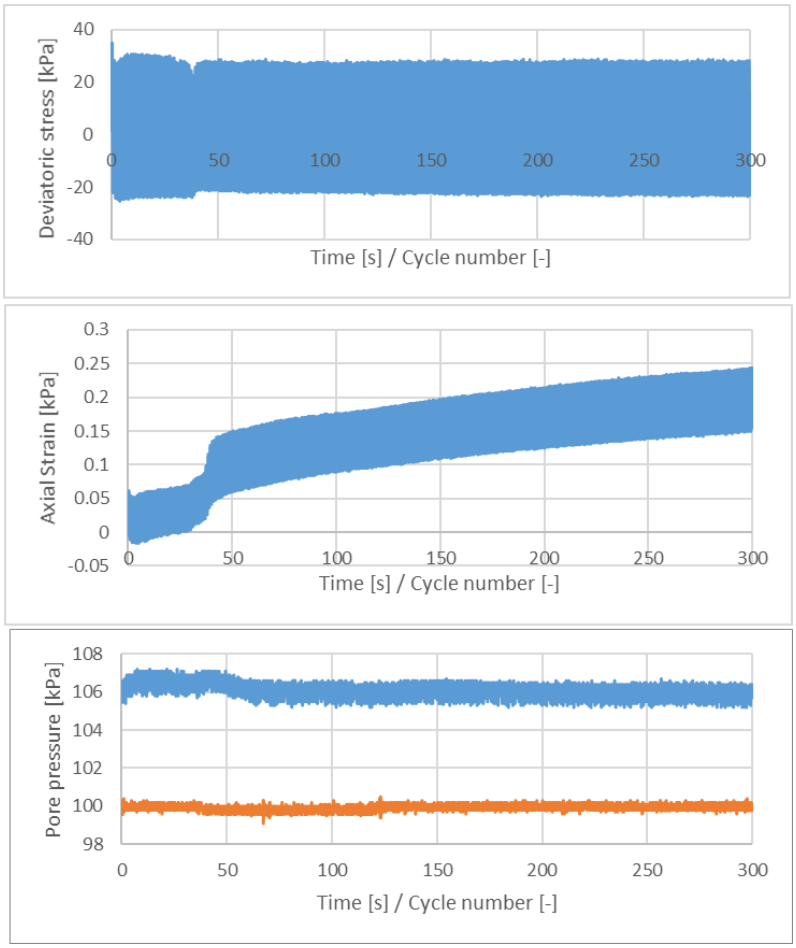

Figure 21 (a) :Deviatoric stress, axial strain and pore pressure during cyclic loading (top t0 bottom) for the untreated samples.

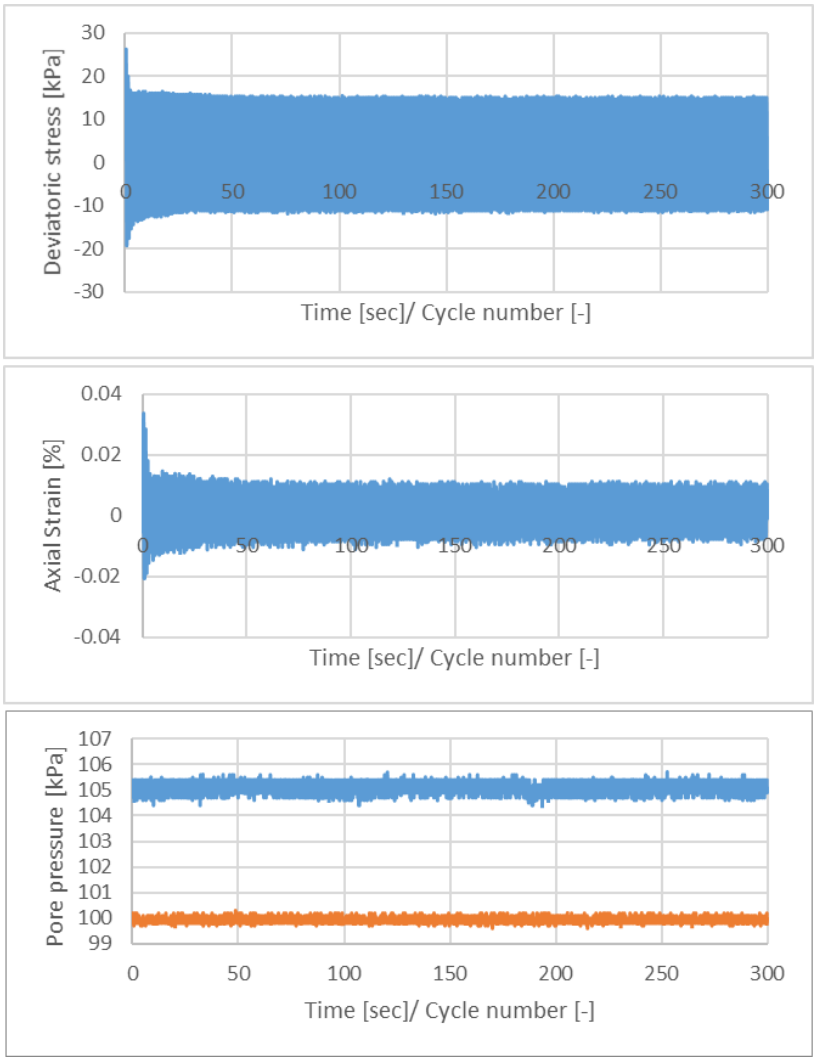

Figure 21 (b):Deviatoric stress, axial strain and pore pressure during cyclic loading (top to bottom) for the treated samples.

The results of the cyclic loading did not show a significant difference between the treated and untreated samples. Although the cyclic stress level was slightly higher in the untreated sample, the axial strains and the pore pressures during each cycle were similar to the treated sample, whereas it was expected that the untreated sample would show a stiffer response and higher pore pressures, due to the compressibility of the gas phase in the treated sample. The untreated sample gradually developed some axial compressive strain, which may be due to asymmetrical load cycle. The deviatoric stress

was alternating between positive and negative values, but the compressive load was slightly higher than the extensive load. Similar asymmetry load cycle of the untreated sample, but that did not lead to any permanent deformation. Still both samples showed very little compaction upon loading, which could be either due to the fact that the load regime changed from a compactional to an extensional regime, or due to the fact the applied load was too low. Additional cyclic loads were applied on the treated sample, but due to an error in the settings, the cyclic deviator stresses were negative, consequently resulting in negative (extensional) strains (Figure 31).

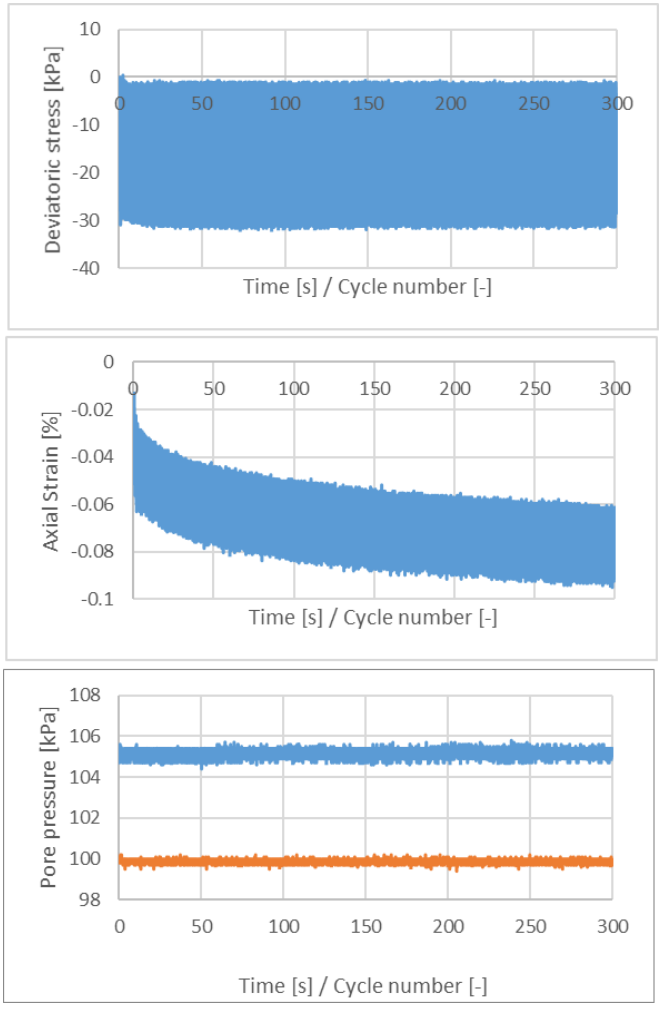

Figure 22 (a): Additional results from (extensional) cyclic loading of the untreated sample: Deviatoric stress, axial strain and pore pressure), for a cyclic load

ranging from 0 to -30 kPa (left) and from -30 to -100 kPa.

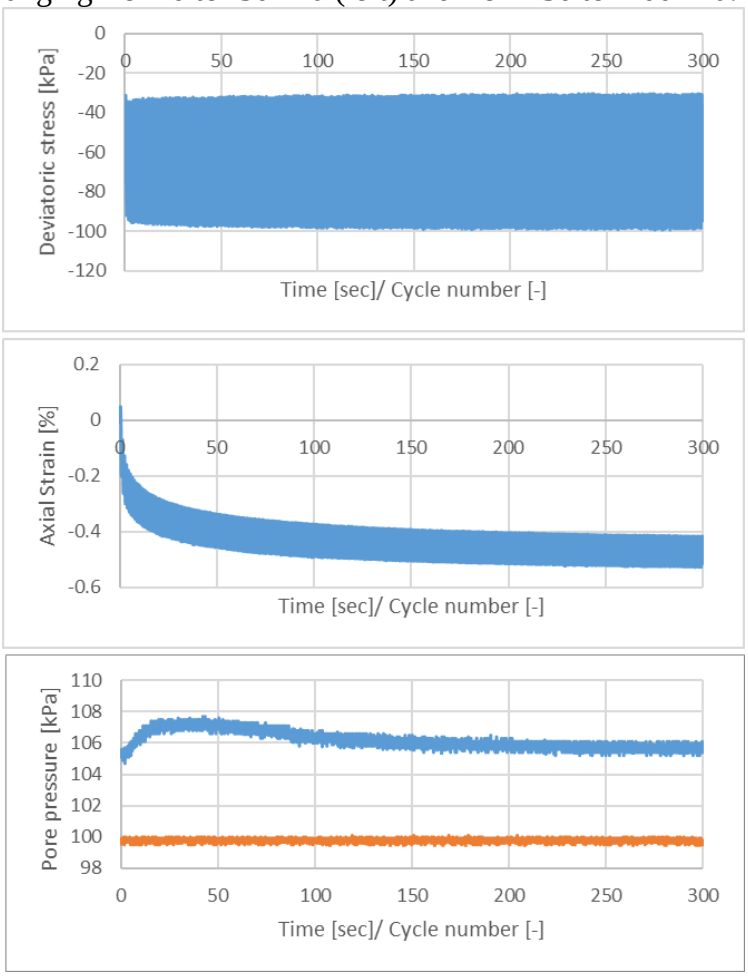

Figure 22 (b): Additional results from (extensional) cyclic loading of the treated sample: Deviatoric stress, axial strain and pore pressure), for a cyclic load ranging from 0 to -30 kPa (left) and from -30 to -100 kPa.

In order to assess the effect of desaturation on the compactibility, a (positive) cyclic compressive axial load should have been applied, instead of a (negative) extenionsal axial load. Hence the hypothesis that desaturation through biogenic gas formation improves the efficiency of dynamic compaction cannot be valadited and additional tests need to be performed with compressive load cycles and higher deviatoric stress levels.

Figure 23: The ASU soil specimen after cyclic triaxial loading

CHAPTER 5

CONCLUSIONS

This entire study has been an attempt to practically verifyif the desaturation of a saturated sand with significant amount of fines helps in the usage of dynamic compaction as a method of densification of the soil. From the tests it was seen that under low confinement condition it the swelling and change in soil volume is directly related to the soil particle size. The ASU soil which had the smallest grain size showed the maximum volume expansion under unconfined conditions while the Ottawa 20-30 sand having the largest grain size among the three soils tested has the least expansion. This raises the question if this swelling potential of the saturated silty sand due to the production of in-situ biogenic gas will affect the overall applicability of the procedure. Therefore the same procedure is now tested under the application of a consolidation pressure. During application of consolidation pressure there is no change in axial strain even in the treated sample. Thus proving that upon the application of a load in-situ gas production will not result in swelling of the soil.

Proof of substantial desaturation of the soil is seen as a result of the production of biogenic gas. Up to 40% desaturation is seen in this case. However only 20% desaturation is sufficient to enable the silty soil to arrive at its maximum dry density. A regulation in the reaction rate and AC/N ratio can help us to achieve that.

However no conclusive result was reached about the effect of biogenic gas production on the compactibility of the soil. The results obtained after the application of the cyclic load did not align with the hypothesis made in the beginning of this study. Hence in the next chapter recommendations have been made regarding future studies that

need to be done on this subject.

This project was based on the recommendations of another similar project done by Gustav Andrag in 2017 titled “Compaction of silty sands through biogenic gas desaturation pre treatment”. At the end of the study the author had inconclusive results and hence was unable to prove his hypothesis. It was suggested that further studies be done on the same hypothesis but with a change in the material within the achievable saturation range be carried out. Adaptations to the test set up and protocol to make the test more representative of the compaction in practice was also suggested. Though these recommendations have been taken into account and the result obtained has positively proven the hypothesis a lot of assumptions were made in this study too.

1. The soil material was assumed to be uniform throughout any test that was carried out.

2. Soil grain particles have been assumed to be spherical for the ease of calculations.

3. Effects of temperature and moisture have been neglected in most tests.

4. The soil parameters of Ottawa 20-30 and F-60 have been collected from existing literature.

5. In the volume expansion tests it is assumed that no gas has left the test set up system.

6. The precipitation of calcite as a product of the chemical reactions has been ignored due to its extremely low production.

7. In the Cyclic triaxial test, the membrane is assumed to be completely impermeable.

8. The value of CSR has been gathered from existing literature, corresponding to the optimum value for dynamic loading capable of doing most harm to a system.

The recommendation for future studies on this hypothesis will be to –

1. Adapt the test system to be reflective of the compaction practices.

2. Corrections for environmental factors such as moisture and temperature must be considered.

3. The precipitation of calcite as a product of the chemical reaction in the inoculums must be taken into account as the calcite has cementing effects which may affect the compressibility of the material.

REFERENCES

Asaka, Y. (2015). Improvement of fine grained reclaimed ground by dynamic compaction method, *15th Asian Regional Conference on Soil Mechanics and Geotechnical Engineering.* 2038-2042

ASTM - D698-07. (2007). Standard Test Methods for Laboratory Compaction Characteristics of Soil Using Standard Effort (12 400 ft-lbf/ft3 (600 kN-m/m3). *American Standards for Testing and Materials*.

ASTM D 5311/D 5311M -13. (2013) Standard Test Method for Load Controlled Cyclic Triaxial Strength of Soil. *American Standards for Testing and Materials*

ASTM D-3999/D3999M - 11$^{\varepsilon 1}$.(2013) Standard Test Methods for the Determination of the Modulus and Damping Properties of Soils Using the Cyclic Triaxial Apparatus. *American Standards for Testing and Materials*.

GCTS Testing Systems (2002). STX-050 Pneumatic Soil Triaxial System. [Brochure]. GCTS Testing Systems, Tempe, Arizona -85281

Ghanbari E., &Hamidi A., (2015) Improvement parameters in dynamic compaction adjacent to slopes. *Journal of Rock Mechanics and Geotechnical Engineering,7,* 233-236

Giovanni C.(2017). Microbially Induced Partial Saturation As Remedial Measure Against Liquefaction: A Review Of Fundamental Concepts. *IncontroAnnualedeiRicercatori di Geotecnica 2017- IARG 2017*

Gustav, G.M. (2017), Compaction of silty sands through biogeic gas desaturation pretreatment, Mastersthesis, Technical University Delft.

Gutierrez A. (2013), The impact of liquefaction on the microstructutre of cohesionless soils, Masters thesis, Arizona State University

He, J. and Chu, J. (2014). Undrained responses of microbiallydesaturated sand under monotonic loading. *Journal of Geotechnical and Geoenvironmental Engineering, 140*(5), 04014003.

He, J., Chu, J., and Liu, H. (2014). Undrained shear strength of desaturated loose sand under monotonic shearing. *Soils and Foundations, 54*(4), 910–916.

Karunawardena A. and Toki M. (2011). Application of the heavy tamping method on Sri Lankan peaty clay for the construction of a highway embankment, *Proc. of the 14th Asian Regional Conference on Soil Mechanics and Geotechnical Engineering,* Paper No. 394

Kavazanjian Jr, E., O'Donnell, S. T., and Hamdan, N. (2015). Biogeotechnical

Mitigation of Earthquake- Induced Soil Liquefaction by Denitrification: A Two Stage Process. In *Proceedings 6ICEGE,* Christchurch, NZ.

Knowles, R. (1982). Denitrification. Microbiological reviews, *46*(1), 43–70.

Lu N. &Likos W. (2006), Suction Stress Characteristic Curve for Unsaturated Soil. *Journal Of Geotechnical And GeoenvironmentalEngineering132*(2): 131-142.

Ménard L., &BroiseY.(1975) Theoretical and practical aspects of dynamic consolidation. *Géotechnique,25*(1), 3-18

Moore J, Mitchell J, MacNeill G, Sutherland B, Lake C (2007).Dynamic compaction of a loose rockfill for the Dartmouth wastewater treatment plant. *Diamond jubilee Canadian geotechnical conference, 8th joint CGS/IAH-CNC groundwater*

O'Donnell Sean, (2016).Mitigation of Earthquake-Induced Soil Liquefaction via Microbial Denitrification: A Two-Stage Process. PhD Thesis, Arizona State University.

Operations Manual HYPROP, UMS.

Pham, V. P. (2017), Bio-based Ground Improvement through Microbial Induced Desaturaion and Precipitation (MIDP), PhD thesis, Technical University Delft.

Pham, V. P., Nakano, A., Van Der Star, W. R. L., Heimovaara, T. J. and Van Paassen, L. A.(2016), Applying MICP by denitrification in soils: a process analysis, *Environmental Geotechnics* 1–15.

Poran CJ, Heh KS, Rodriguez JA (1992) Impact behavior of sand. *Soils Found 32*(4):81–92

Rebata-Landa, V. and Santamarina, J. C. (2012). Mechanical effects of biogenic nitrogen gas bubbles in soils.*Journal of Geotechnical and Geoenvironmental Engineering*, *138*(2), 128–137.

Schindler, U., Durner, W.,von Unold, G., Müller, L. and Wieland, R. (2010b): The evaporation method: Extending the measurement range of soil hydraulic properties using the air entry pressure of the ceramic cup. *Journal of Plant Nutrition and Soil Science 173 (4):* 563-572.

Seed, H.B. and Idriss, I.M. (1971) Simplified Procedure for Evaluating Soil Liquefaction Potential. *Journal of the Soil Mechanics and Foundations Division, 97,* 1249-1273.

Terzaghi K, Peck RB (1948) Soil mechanics in engineering, practice.*Wiley, New York*

van Paassen, L. A., Daza, C. M., Staal, M., Sorokin, D. Y., Van Der Zon, W. H. and van Loosdrecht, M. C. M. (2010). Potential soil reinforcement by biological denitrification, *Ecological Engineering 36*(2), 168–175.

van Paassen, L. A., Pham V., Mahabadi, N., Hall, C., Stallings, E. and Kavazanjian Jr.,E. (2018). Desaturation via Biogenic Gas Formation as a Ground ImprovementTechnique, *PanAm Unsaturated Soils 2017 GSP 300*, 244-256.

van Spanning, R. J. M., Richards, D. J. and Ferguson, S. J. (2006), Introduction to the Biochemistry and Molecular Biology of Denitrification, in H. Bothe, S. Ferguson and W. Newton, eds, *Biology of the Nitrogen Cycle,0,* 1, xiii–20

Wheeler, S. J. 1990. Movement of large gas bubbles in unsaturated fine-grained sediments. *Marine Geotechnology 9*(2): 113–129.

Whiffin, V. S. (2004). Microbial CaCO3 precipitation for the production ofBiocement. PhD Dissertation,Murdoch University, Western Australia

Yogendrakumar M, Wedge N (2014) Design and construction of the new Coal Harbour shoreline in downtown Vancouver. *22nd Symposium of the Vancouver geotechnical society, Foreshore Engineering, Vancouver*

APPENDIX A

ALL DATA COLLECTED FOR VARIOUS TESTS FROM NOVEMBER 2017- JUNE 2018

Table 3–Results of dry sieving of the ASU soil

1	2	3	4	5	6	7	8
Sieve No.	**Mesh size (mm)**	**Mass of sieve (g)**	**Mass of sieve+soil retained (g)**	**Mass of soil retained (Column 4-Column 5) (g)**	**Cumulative mass retained (g)**	**% Retained (Column 6/1931g)*100**	**% Finer (100-Column 7)**
4	4.75	451.8	560.7	108.9	108.9	5.639565	94.360435
5	4	494.1	504.7	10.6	119.5	6.1885034	93.811497
8	2.38	470.2	513.8	43.6	163.1	8.4464008	91.553599
10	2	429.4	446.2	16.8	179.9	9.3164164	90.683584
16	1.19	343.3	393.5	50.2	230.1	11.916106	88.083894
20	0.841	468.3	509.4	41.1	271.2	14.044537	85.955463
30	0.6	366.4	429.6	63.2	334.4	17.317452	82.682548
40	0.425	356.8	482.2	125.4	459.8	23.811497	76.188503
60	0.25	359.5	1005.4	645.9	1105.7	57.260487	42.739513
100	0.15	359.3	717.7	358.4	1464.1	75.820818	24.179182
200	0.075	309.3	645.9	336.6	1800.7	93.252201	6.7477991
Pan		480.7	611	130.3	1931	100	0

Table 4: Results of wet sieving of ASU soil

1	2	3	4	5	6	7	8
Sieve No.	**Mesh size (mm)**	**Mass of sieve (g)**	**Mass of sieve+soil retained (g)**	**Mass of soil retained (Column 4-Column 5) (g)**	**Cumulative mass retained (g)**	**% Retained (Column 6/1931g)*100**	**% Finer (100-Column 7)**
4	4.75	451.8	504.8	53	53	2.7	97.3
5	4	494.1	496.8	2.7	55.7	2.9	97.1
8	2.38	470.2	480	9.8	65.5	3.4	96.6
10	2	429.4	432.7	3.3	68.8	3.6	96.4
16	1.19	343.3	359.6	16.3	85.1	4.4	95.6
20	0.841	468.3	488.1	19.8	104.9	5.4	94.6
30	0.6	366.4	406.1	39.7	144.6	7.5	92.5
40	0.425	356.8	457.2	100.4	245	12.7	87.3
60	0.25	359.5	668.4	308.9	554	28.7	71.3
100	0.15	359.3	894.0	534.7	1089	56.4	43.6
200	0.075	309.3	671.7	362.4	1451	75.1	24.9
Pan		480.7	957.0	476.3	1927	99.8	0.2

The highlighted portion of the wet sieving shows the portion of the soil which passes the No. 40 sieve. 245 g of soil was retained above No. 40 soil and 1682 g of soil passed No. 40 sieve during wet sieving.

Table 5 : Results of liquid limit test of ASU soil

Test no.	**1**	**2**	**3**	**4**
No. Of blows (N)	8	21	33	57
Can no.	2	3	4	5
Mass of can, M1 (g)	14.36	14.3	14.76	14.33
Mass of can + moist soil, M2 (g)	20.2	21.54	24.12	21.2
Mass of can + dry soil, M3 (g)	18.56	19.56	21.64	19.43
Moisture content, w% = ((M2-M3)/(M3-M1))*100	39.05	37.64	36.046	34.70

Table 6: Results of Standard Proctor Test of ASU soil

Initial moisture content (%)	0.015	0.09	0.12	0.15	0.18
Total soil (g)	3000	3100	3096.5	3094	3013
Water to be added %	9	12	15	18	21
Weight of water to be added (gm)	221.674877	85.321101	82.9419643	80.713043	76.6016949
Volume of the cylinder (cc)	936.15	936.15	936.15	936.15	936.15
Wt of the cylinder without base plate	2013.9	2013.9	2013.9	2013.9	2013.9
Wt of the cylinder + compacted soil (gm)	3807	3901.7	3991.9	3987	3954.6
Weight of the compacted soil (gm)	1793.1	1887.8	1978	1973.1	1940.7
Wet density (gm/cc)	1.91539817	2.0165572	2.11290926	2.1076751	2.07306521
Container No.	1	2	3	4	5
Weight of container	14.37	13.97	14.23	14.93	14.14
Weight of container +wet soil	34.8	41.37	52.49	47.61	48.96
Weight of container +dry soil	33.24	38.71	48.28	43.31	43.87
Water content	8.26709062	10.751819	12.3641703	15.151515	17.1207534
Dry density (gm/cc)	1.76914163	1.8207892	1.88041192	1.8303494	1.7700238

Table 7 :Change in the volume and void ratio of the ASU Soil with time

		Column 1 Treated			Column 2 Treated			Control Untreated	
Time (hours)	**Volume of soil (cm3)**	**Volume of solids (cm3)**	**Void ratio**	**Volume of soil (cm3)**	**Volume of solids (cm3)**	**Void ratio**	**Volume of soil (cm3)**	**Volume of solids**	**Void ratio**
0	635	421.585	0.51	499	350.765	0.42	515	355.19	0.45
0.5	630	421.585	0.49	499	350.765	0.42	515	355.19	0.45
1	628	421.585	0.49	499	350.765	0.42	515	355.19	0.45
1.5	628	421.585	0.49	500	350.765	0.43	515	355.19	0.45
2	627	421.585	0.49	500	350.765	0.43	515	355.19	0.45
2.5	625	421.585	0.48	500	350.765	0.43	515	355.19	0.45
3	624	421.585	0.48	500	350.765	0.43	515	355.19	0.45
3.5	624	421.585	0.48	500	350.765	0.43	515	355.19	0.45
4	624	421.585	0.48	500	350.765	0.43	515	355.19	0.45
4.5	622	421.585	0.48	500	350.765	0.43	515	355.19	0.45
5	621	421.585	0.47	502	350.765	0.43	515	355.19	0.45
5.5	621	421.585	0.47	502	350.765	0.43	515	355.19	0.45
6	621	421.585	0.47	505	350.765	0.44	515	355.19	0.45
6.5	625	421.585	0.48	505	350.765	0.44	515	355.19	0.45
7	629	421.585	0.49	505	350.765	0.44	515	355.19	0.45
7.5	630	421.585	0.49	510	350.765	0.45	515	355.19	0.45
8	630	421.585	0.49	511	350.765	0.46	515	355.19	0.45
8.5	630	421.585	0.49	512	350.765	0.46	515	355.19	0.45
9	630	421.585	0.49	520	350.765	0.48	515	355.19	0.45
9.5	630	421.585	0.49	520	350.765	0.48	515	355.19	0.45
10	630	421.585	0.49	530	350.765	0.51	515	355.19	0.45
10.5	631	421.585	0.50	530	350.765	0.51	515	355.19	0.45
11	632	421.585	0.50	540	350.765	0.54	515	355.19	0.45
11.5	634	421.585	0.50	540	350.765	0.54	515	355.19	0.45
12	635	421.585	0.51	550	350.765	0.57	515	355.19	0.45
12.5	639	421.585	0.52	560	350.765	0.60	515	355.19	0.45
13	640	421.585	0.52	570	350.765	0.63	515	355.19	0.45
13.5	641	421.585	0.52	580	350.765	0.65	515	355.19	0.45
14	645	421.585	0.53	590	350.765	0.68	515	355.19	0.45
14.5	650	421.585	0.54	600	350.765	0.71	515	355.19	0.45
15	652	421.585	0.55	610	350.765	0.74	515	355.19	0.45
15.5	655	421.585	0.55	630	350.765	0.80	515	355.19	0.45
16	662	421.585	0.57	640	350.765	0.82	515	355.19	0.45
16.5	670	421.585	0.59	642	350.765	0.83	515	355.19	0.45

17	680	421.585	0.61	630	350.765	0.80	515	355.19	0.45
17.5	690	421.585	0.64	635	350.765	0.81	515	355.19	0.45
18	695	421.585	0.65	645	350.765	0.84	515	355.19	0.45
18.5	700	421.585	0.66	650	350.765	0.85	515	355.19	0.45
19	710	421.585	0.68	651	350.765	0.86	515	355.19	0.45
19.5	720	421.585	0.71	651	350.765	0.86	515	355.19	0.45
20	730	421.585	0.73	652	350.765	0.86	515	355.19	0.45
20.5	750	421.585	0.78	655	350.765	0.87	515	355.19	0.45
21	760	421.585	0.80	655	350.765	0.87	515	355.19	0.45
21.5	765	421.585	0.81	655	350.765	0.87	515	355.19	0.45
22	767	421.585	0.82	660	350.765	0.88	515	355.19	0.45
22.5	770	421.585	0.83	660	350.765	0.88	515	355.19	0.45
23	770	421.585	0.83	661	350.765	0.88	515	355.19	0.45
23.5	770	421.585	0.83	660	350.765	0.88	515	355.19	0.45
24	770	421.585	0.83	662	350.765	0.89	515	355.19	0.45
24.5	772	421.585	0.83	663	350.765	0.89	515	355.19	0.45
25	772	421.585	0.83	662	350.765	0.89	515	355.19	0.45
25.5	772	421.585	0.83	665	350.765	0.90	515	355.19	0.45
26	772	421.585	0.83	665	350.765	0.90	515	355.19	0.45
26.5	775	421.585	0.84	665	350.765	0.90	515	355.19	0.45
27	775	421.585	0.84	666	350.765	0.90	515	355.19	0.45
27.5	775	421.585	0.84	668	350.765	0.90	515	355.19	0.45
28	780	421.585	0.85	670	350.765	0.91	515	355.19	0.45
28.5	780	421.585	0.85	670	350.765	0.91	515	355.19	0.45
29	780	421.585	0.85	670	350.765	0.91	515	355.19	0.45
29.5	780	421.585	0.85	670	350.765	0.91	515	355.19	0.45
30	781	421.585	0.85	670	350.765	0.91	515	355.19	0.45
30.5	781	421.585	0.85	670	350.765	0.91	515	355.19	0.45
31	785	421.585	0.86	670	350.765	0.91	515	355.19	0.45
31.5	786	421.585	0.86	670	350.765	0.91	515	355.19	0.45
32	787	421.585	0.87	670	350.765	0.91	515	355.19	0.45
32.5	785	421.585	0.86	670	350.765	0.91	515	355.19	0.45
33	785	421.585	0.86	671	350.765	0.91	515	355.19	0.45
33.5	785	421.585	0.86	672	350.765	0.92	515	355.19	0.45
34	787	421.585	0.87	675	350.765	0.92	515	355.19	0.45
34.5	787	421.585	0.87	676	350.765	0.93	515	355.19	0.45
35	790	421.585	0.87	677	350.765	0.93	515	355.19	0.45

Table 8 :Change in the volume and void ratio of three different soils

		F-60 soil			Ottowa 20-30			ASU Soil	
Time (hours)	Volume of the soil (cm3)	Volume of solids (cm3)	Void ratio	Volume of the soil (cm3)	Volume of solids (cm3)	Void ratio	Volume of the soil (cm3)	Volume of solids (cm3)	Void ratio
0	475	288.91	0.64	462	286.79	0.611	500	274.59	0.82
0.5	475	288.91	0.64	462	286.79	0.611	500	274.59	0.82
1	475	288.91	0.64	462	286.79	0.611	500	274.59	0.82
1.5	474	288.91	0.64	462	286.79	0.611	500	274.59	0.82
2	473	288.91	0.64	462	286.79	0.611	500	274.59	0.82
2.5	473	288.91	0.64	462	286.79	0.611	500	274.59	0.82
3	473	288.91	0.64	462	286.79	0.611	500	274.59	0.82
3.5	472	288.91	0.63	465	286.79	0.621	500	274.59	0.82
4	472	288.91	0.63	465	286.79	0.621	500	274.59	0.82
4.5	472	288.91	0.63	465	286.79	0.621	500	274.59	0.82
5	472	288.91	0.63	470	286.79	0.639	500	274.59	0.82
5.5	472	288.91	0.63	470	286.79	0.639	500	274.59	0.82
6	472	288.91	0.63	470	286.79	0.639	501	274.59	0.82
6.5	471	288.91	0.63	470	286.79	0.639	505	274.59	0.84
7	471	288.91	0.63	470	286.79	0.639	505	274.59	0.84
7.5	471	288.91	0.63	470	286.79	0.639	507	274.59	0.85
8	471	288.91	0.63	470	286.79	0.639	508	274.59	0.85
8.5	471	288.91	0.63	470	286.79	0.639	510	274.59	0.86
9	471	288.91	0.63	470	286.79	0.639	510	274.59	0.86
9.5	471	288.91	0.63	470	286.79	0.639	510	274.59	0.86
10	471	288.91	0.63	470	286.79	0.639	512	274.59	0.86
10.5	471	288.91	0.63	472	286.79	0.646	512	274.59	0.86
11	471	288.91	0.63	472	286.79	0.646	513	274.59	0.87
11.5	471	288.91	0.63	475	286.79	0.656	515	274.59	0.88
12	471	288.91	0.63	480	286.79	0.674	518	274.59	0.89
12.5	471	288.91	0.63	480	286.79	0.674	520	274.59	0.89
13	470	288.91	0.63	480	286.79	0.674	521	274.59	0.90
13.5	470	288.91	0.63	480	286.79	0.674	525	274.59	0.91
14	470	288.91	0.63	480	286.79	0.674	530	274.59	0.93
14.5	470	288.91	0.63	480	286.79	0.674	532	274.59	0.94

15	470	288.91	0.63	480	286.79	0.674	535	274.59	0.95
15.5	470	288.91	0.63	480	286.79	0.674	540	274.59	0.97
16	470	288.91	0.63	480	286.79	0.674	545	274.59	0.98
16.5	470	288.91	0.63	480	286.79	0.674	540	274.59	0.97
17	470	288.91	0.63	480	286.79	0.674	545	274.59	0.98
17.5	470	288.91	0.63	480	286.79	0.674	550	274.59	1.00
18	470	288.91	0.63	480	286.79	0.674	560	274.59	1.04
18.5	470	288.91	0.63	480	286.79	0.674	565	274.59	1.06
19	470	288.91	0.63	480	286.79	0.674	570	274.59	1.08
19.5	470	288.91	0.63	480	286.79	0.674	580	274.59	1.11
20	470	288.91	0.63	480	286.79	0.674	590	274.59	1.15
20.5	470	288.91	0.63	480	286.79	0.674	590	274.59	1.15
21	470	288.91	0.63	480	286.79	0.674	590	274.59	1.15
21.5	470	288.91	0.63	480	286.79	0.674	600	274.59	1.19
22	470	288.91	0.63	480	286.79	0.674	610	274.59	1.22
22.5	470	288.91	0.63	480	286.79	0.674	630	274.59	1.29
23	470	288.91	0.63	480	286.79	0.674	620	274.59	1.26
23.5	470	288.91	0.63	480	286.79	0.674	620	274.59	1.26
24	470	288.91	0.63	480	286.79	0.674	620	274.59	1.26
24.5	470	288.91	0.63	485	286.79	0.691	625	274.59	1.28
25	470	288.91	0.63	485	286.79	0.691	620	274.59	1.26
25.5	470	288.91	0.63	485	286.79	0.691	620	274.59	1.26
26	470	288.91	0.63	485	286.79	0.691	620	274.59	1.26
26.5	470	288.91	0.63	485	286.79	0.691	630	274.59	1.29
27	470	288.91	0.63	485	286.79	0.691	630	274.59	1.29
27.5	470	288.91	0.63	485	286.79	0.691	630	274.59	1.29
28	470	288.91	0.63	485	286.79	0.691	630	274.59	1.29
28.5	470	288.91	0.63	485	286.79	0.691	630	274.59	1.29
29	470	288.91	0.63	485	286.79	0.691	640	274.59	1.33
29.5	471	288.91	0.63	485	286.79	0.691	640	274.59	1.33
30	471	288.91	0.63	485	286.79	0.691	640	274.59	1.33
30.5	471	288.91	0.63	485	286.79	0.691	640	274.59	1.33
31	471	288.91	0.63	485	286.79	0.691	650	274.59	1.37
31.5	471	288.91	0.63	485	286.79	0.691	640	274.59	1.33
32	471	288.91	0.63	485	286.79	0.691	660	274.59	1.40
32.5	471	288.91	0.63	485	286.79	0.691	650	274.59	1.37

33	471	288.91	0.63	485	286.79	0.691	650	274.59	1.37
33.5	472	288.91	0.63	485	286.79	0.691	650	274.59	1.37
34	472	288.91	0.63	485	286.79	0.691	650	274.59	1.37
34.5	472	288.91	0.63	485	286.79	0.691	650	274.59	1.37
35	474	288.91	0.64	485	286.79	0.691	650	274.59	1.37
35.5	475	288.91	0.64	485	286.79	0.691	650	274.59	1.37
36	476	288.91	0.65	490	286.79	0.709	650	274.59	1.37
36.5	476	288.91	0.65	490	286.79	0.709	650	274.59	1.37
37	477	288.91	0.65	490	286.79	0.709	650	274.59	1.37
37.5	478	288.91	0.65	490	286.79	0.709	650	274.59	1.37
38	480	288.91	0.66	490	286.79	0.709	650	274.59	1.37
38.5	480	288.91	0.66	490	286.79	0.709	650	274.59	1.37
39	480	288.91	0.66	490	286.79	0.709	650	274.59	1.37
39.5	480	288.91	0.66	490	286.79	0.709	650	274.59	1.37
40	480	288.91	0.66	490	286.79	0.709	650	274.59	1.37
40.5	480	288.91	0.66	490	286.79	0.709	650	274.59	1.37
41	481	288.91	0.66	490	286.79	0.709	650	274.59	1.37
41.5	482	288.91	0.67	490	286.79	0.709	650	274.59	1.37
42	485	288.91	0.68	490	286.79	0.709	650	274.59	1.37
42.5	490	288.91	0.70	490	286.79	0.709	650	274.59	1.37
43	490	288.91	0.70	490	286.79	0.709	650	274.59	1.37
43.5	490	288.91	0.70	490	286.79	0.709	650	274.59	1.37
44	492	288.91	0.70	490	286.79	0.709	650	274.59	1.37
44.5	495	288.91	0.71	490	286.79	0.709	650	274.59	1.37
45	500	288.91	0.73	490	286.79	0.709	650	274.59	1.37
45.5	500	288.91	0.73	490	286.79	0.709	650	274.59	1.37
46	500	288.91	0.73	490	286.79	0.709	650	274.59	1.37
46.5	500	288.91	0.73	490	286.79	0.709	650	274.59	1.37
47	510	288.91	0.77	490	286.79	0.709	650	274.59	1.37
47.5	510	288.91	0.77	485	286.79	0.691	650	274.59	1.37
48	505	288.91	0.75	485	286.79	0.691	650	274.59	1.37
48.5	505	288.91	0.75	485	286.79	0.691	650	274.59	1.37
49	505	288.91	0.75	485	286.79	0.691	650	274.59	1.37
49.5	505	288.91	0.75	485	286.79	0.691	650	274.59	1.37
50	505	288.91	0.75	485	286.79	0.691	650	274.59	1.37
50.5	512	288.91	0.77	485	286.79	0.691	650	274.59	1.37

51	515	288.91	0.78	485	286.79	0.691	650	274.59	1.37
51.5	520	288.91	0.80	485	286.79	0.691	650	274.59	1.37
52	520	288.91	0.80	485	286.79	0.691	650	274.59	1.37
52.5	520	288.91	0.80	485	286.79	0.691	650	274.59	1.37
53	520	288.91	0.80	485	286.79	0.691	650	274.59	1.37
53.5	520	288.91	0.80	485	286.79	0.691	650	274.59	1.37
54	520	288.91	0.80	485	286.79	0.691	650	274.59	1.37
54.5	515	288.91	0.78	485	286.79	0.691	650	274.59	1.37
55	510	288.91	0.77	485	286.79	0.691	650	274.59	1.37
55.5	510	288.91	0.77	485	286.79	0.691	650	274.59	1.37
56	512	288.91	0.77	480	286.79	0.674	650	274.59	1.37
56.5	520	288.91	0.80	480	286.79	0.674	650	274.59	1.37
57	520	288.91	0.80	480	286.79	0.674	650	274.59	1.37
57.5	520	288.91	0.80	480	286.79	0.674	650	274.59	1.37
58	525	288.91	0.82	480	286.79	0.674	650	274.59	1.37
58.5	525	288.91	0.82	480	286.79	0.674	650	274.59	1.37
59	530	288.91	0.83	480	286.79	0.674	650	274.59	1.37
59.5	530	288.91	0.83	480	286.79	0.674	650	274.59	1.37
60	530	288.91	0.83	480	286.79	0.674	650	274.59	1.37
60.5	530	288.91	0.83	480	286.79	0.674	650	274.59	1.37
61	535	288.91	0.85	480	286.79	0.674	650	274.59	1.37
61.5	535	288.91	0.85	480	286.79	0.674	650	274.59	1.37
62	535	288.91	0.85	480	286.79	0.674	650	274.59	1.37
62.5	540	288.91	0.87	480	286.79	0.674	650	274.59	1.37
63	540	288.91	0.87	480	286.79	0.674	650	274.59	1.37
63.5	540	288.91	0.87	480	286.79	0.674	650	274.59	1.37
64	540	288.91	0.87	480	286.79	0.674	650	274.59	1.37
64.5	540	288.91	0.87	480	286.79	0.674	650	274.59	1.37
65	535	288.91	0.85	480	286.79	0.674	650	274.59	1.37
65.5	530	288.91	0.83	480	286.79	0.674	650	274.59	1.37
66	530	288.91	0.83	480	286.79	0.674	650	274.59	1.37
66.5	532	288.91	0.84	480	286.79	0.674	650	274.59	1.37
67	532	288.91	0.84	480	286.79	0.674	650	274.59	1.37
67.5	532	288.91	0.84	480	286.79	0.674	650	274.59	1.37
68	532	288.91	0.84	480	286.79	0.674	640	274.59	1.33
68.5	532	288.91	0.84	480	286.79	0.674	640	274.59	1.33

69	532	288.91	0.84	480	286.79	0.674	640	274.59	1.33
69.5	532	288.91	0.84	480	286.79	0.674	640	274.59	1.33
70	532	288.91	0.84	480	286.79	0.674	640	274.59	1.33
70.5	532	288.91	0.84	480	286.79	0.674	640	274.59	1.33
71	532	288.91	0.84	480	286.79	0.674	640	274.59	1.33
71.5	535	288.91	0.85	480	286.79	0.674	640	274.59	1.33
72	540	288.91	0.87	480	286.79	0.674	640	274.59	1.33
72.5	532	288.91	0.84	480	286.79	0.674	640	274.59	1.33
73	532	288.91	0.84	480	286.79	0.674	640	274.59	1.33
73.5	532	288.91	0.84	480	286.79	0.674	640	274.59	1.33
74	532	288.91	0.84	480	286.79	0.674	640	274.59	1.33
74.5	532	288.91	0.84	480	286.79	0.674	640	274.59	1.33
75	532	288.91	0.84	480	286.79	0.674	640	274.59	1.33
75.5	532	288.91	0.84	480	286.79	0.674	640	274.59	1.33
76	532	288.91	0.84	480	286.79	0.674	640	274.59	1.33
76.5	532	288.91	0.84	480	286.79	0.674	640	274.59	1.33
77	532	288.91	0.84	480	286.79	0.674	640	274.59	1.33
77.5	532	288.91	0.84	480	286.79	0.674	640	274.59	1.33
78	532	288.91	0.84	480	286.79	0.674	640	274.59	1.33
78.5	532	288.91	0.84	480	286.79	0.674	640	274.59	1.33
79	532	288.91	0.84	480	286.79	0.674	640	274.59	1.33
79.5	532	288.91	0.84	480	286.79	0.674	640	274.59	1.33
80	532	288.91	0.84	480	286.79	0.674	640	274.59	1.33
80.5	532	288.91	0.84	480	286.79	0.674	640	274.59	1.33
81	532	288.91	0.84	480	286.79	0.674	640	274.59	1.33
81.5	532	288.91	0.84	480	286.79	0.674	640	274.59	1.33
82	532	288.91	0.84	480	286.79	0.674	640	274.59	1.33
82.5	532	288.91	0.84	480	286.79	0.674	640	274.59	1.33
83	532	288.91	0.84	480	286.79	0.674	640	274.59	1.33
83.5	532	288.91	0.84	480	286.79	0.674	640	274.59	1.33
84	532	288.91	0.84	480	286.79	0.674	640	274.59	1.33
84.5	532	288.91	0.84	480	286.79	0.674	640	274.59	1.33
85	532	288.91	0.84	480	286.79	0.674	640	274.59	1.33
85.5	532	288.91	0.84	480	286.79	0.674	640	274.59	1.33
86	532	288.91	0.84	480	286.79	0.674	640	274.59	1.33
86.5	532	288.91	0.84	480	286.79	0.674	640	274.59	1.33

87	532	288.91	0.84	480	286.79	0.674	640	274.59	1.33
87.5	532	288.91	0.84	480	286.79	0.674	640	274.59	1.33
88	532	288.91	0.84	480	286.79	0.674	640	274.59	1.33
88.5	532	288.91	0.84	480	286.79	0.674	640	274.59	1.33
89	532	288.91	0.84	480	286.79	0.674	640	274.59	1.33
89.5	532	288.91	0.84	480	286.79	0.674	640	274.59	1.33
90	532	288.91	0.84	480	286.79	0.674	640	274.59	1.33
90.5	532	288.91	0.84	480	286.79	0.674	640	274.59	1.33
91	532	288.91	0.84	480	286.79	0.674	640	274.59	1.33
91.5	532	288.91	0.84	480	286.79	0.674	640	274.59	1.33
92	532	288.91	0.84	480	286.79	0.674	640	274.59	1.33
92.5	532	288.91	0.84	480	286.79	0.674	640	274.59	1.33
93	532	288.91	0.84	480	286.79	0.674	640	274.59	1.33
93.5	532	288.91	0.84	480	286.79	0.674	640	274.59	1.33
94	532	288.91	0.84	480	286.79	0.674	640	274.59	1.33
94.5	532	288.91	0.84	480	286.79	0.674	640	274.59	1.33
95	532	288.91	0.84	480	286.79	0.674	640	274.59	1.33
95.5	532	288.91	0.84	480	286.79	0.674	650	274.59	1.37
96	532	288.91	0.84	480	286.79	0.674	650	274.59	1.37
96.5	532	288.91	0.84	480	286.79	0.674	650	274.59	1.37
97	532	288.91	0.84	480	286.79	0.674	650	274.59	1.37
97.5	532	288.91	0.84	480	286.79	0.674	650	274.59	1.37
98	532	288.91	0.84	480	286.79	0.674	650	274.59	1.37
98.5	532	288.91	0.84	480	286.79	0.674	650	274.59	1.37
99	532	288.91	0.84	480	286.79	0.674	650	274.59	1.37
99.5	532	288.91	0.84	480	286.79	0.674	650	274.59	1.37
100	532	288.91	0.84	480	286.79	0.674	650	274.59	1.37
100.5	532	288.91	0.84	480	286.79	0.674	650	274.59	1.37
101	532	288.91	0.84	480	286.79	0.674	650	274.59	1.37
101.5	532	288.91	0.84	480	286.79	0.674	650	274.59	1.37
102	532	288.91	0.84	480	286.79	0.674	650	274.59	1.37
102.5	532	288.91	0.84	480	286.79	0.674	650	274.59	1.37
103	532	288.91	0.84	480	286.79	0.674	650	274.59	1.37
103.5	532	288.91	0.84	480	286.79	0.674	650	274.59	1.37
104	532	288.91	0.84	480	286.79	0.674	650	274.59	1.37
104.5	532	288.91	0.84	480	286.79	0.674	650	274.59	1.37

105	532	288.91	0.84	480	286.79	0.674	650	274.59	1.37
105.5	532	288.91	0.84	480	286.79	0.674	650	274.59	1.37
106	532	288.91	0.84	480	286.79	0.674	650	274.59	1.37
106.5	532	288.91	0.84	480	286.79	0.674	650	274.59	1.37
107	532	288.91	0.84	480	286.79	0.674	650	274.59	1.37
107.5	532	288.91	0.84	480	286.79	0.674	650	274.59	1.37
108	532	288.91	0.84	480	286.79	0.674	650	274.59	1.37
108.5	532	288.91	0.84	480	286.79	0.674	650	274.59	1.37
109	532	288.91	0.84	480	286.79	0.674	650	274.59	1.37
109.5	532	288.91	0.84	480	286.79	0.674	650	274.59	1.37
110	532	288.91	0.84	480	286.79	0.674	650	274.59	1.37
110.5	532	288.91	0.84	480	286.79	0.674	650	274.59	1.37
111	532	288.91	0.84	480	286.79	0.674	650	274.59	1.37
111.5	532	288.91	0.84	480	286.79	0.674	650	274.59	1.37
112	532	288.91	0.84	480	286.79	0.674	650	274.59	1.37
112.5	532	288.91	0.84	480	286.79	0.674	650	274.59	1.37
113	532	288.91	0.84	480	286.79	0.674	650	274.59	1.37
113.5	532	288.91	0.84	480	286.79	0.674	650	274.59	1.37
114	532	288.91	0.84	480	286.79	0.674	650	274.59	1.37
114.5	532	288.91	0.84	480	286.79	0.674	650	274.59	1.37
115	532	288.91	0.84	480	286.79	0.674	650	274.59	1.37
115.5	532	288.91	0.84	480	286.79	0.674	650	274.59	1.37
116	532	288.91	0.84	480	286.79	0.674	650	274.59	1.37
116.5	532	288.91	0.84	480	286.79	0.674	650	274.59	1.37
117	532	288.91	0.84	480	286.79	0.674	650	274.59	1.37
117.5	532	288.91	0.84	480	286.79	0.674	650	274.59	1.37
118	532	288.91	0.84	480	286.79	0.674	650	274.59	1.37
118.5	532	288.91	0.84	480	286.79	0.674	650	274.59	1.37
119	532	288.91	0.84	480	286.79	0.674	650	274.59	1.37
119.5	532	288.91	0.84	480	286.79	0.674	650	274.59	1.37
120	532	288.91	0.84	480	286.79	0.674	650	274.59	1.37
120.5	532	288.91	0.84	480	286.79	0.674	650	274.59	1.37
121	532	288.91	0.84	480	286.79	0.674	650	274.59	1.37
121.5	532	288.91	0.84	480	286.79	0.674	650	274.59	1.37
122	532	288.91	0.84	480	286.79	0.674	650	274.59	1.37
122.5	532	288.91	0.84	480	286.79	0.674	650	274.59	1.37

123	532	288.91	0.84	480	286.79	0.674	650	274.59	1.37
123.5	532	288.91	0.84	480	286.79	0.674	650	274.59	1.37
124	532	288.91	0.84	480	286.79	0.674	650	274.59	1.37
124.5	532	288.91	0.84	480	286.79	0.674	650	274.59	1.37
125	532	288.91	0.84	480	286.79	0.674	650	274.59	1.37
125.5	532	288.91	0.84	480	286.79	0.674	650	274.59	1.37
126	532	288.91	0.84	480	286.79	0.674	650	274.59	1.37
126.5	532	288.91	0.84	480	286.79	0.674	650	274.59	1.37
127	532	288.91	0.84	480	286.79	0.674	650	274.59	1.37
127.5	532	288.91	0.84	480	286.79	0.674	650	274.59	1.37
128	532	288.91	0.84	480	286.79	0.674	650	274.59	1.37
128.5	532	288.91	0.84	480	286.79	0.674	650	274.59	1.37
129	532	288.91	0.84	480	286.79	0.674	650	274.59	1.37
129.5	532	288.91	0.84	480	286.79	0.674	650	274.59	1.37
130	532	288.91	0.84	480	286.79	0.674	650	274.59	1.37
130.5	532	288.91	0.84	480	286.79	0.674	650	274.59	1.37
131	532	288.91	0.84	480	286.79	0.674	650	274.59	1.37
131.5	532	288.91	0.84	480	286.79	0.674	650	274.59	1.37
132	532	288.91	0.84	480	286.79	0.674	650	274.59	1.37
132.5	532	288.91	0.84	480	286.79	0.674	650	274.59	1.37
133	532	288.91	0.84	480	286.79	0.674	650	274.59	1.37
133.5	532	288.91	0.84	480	286.79	0.674	650	274.59	1.37
134	532	288.91	0.84	480	286.79	0.674	650	274.59	1.37
134.5	532	288.91	0.84	480	286.79	0.674	650	274.59	1.37
135	532	288.91	0.84	480	286.79	0.674	650	274.59	1.37
135.5	532	288.91	0.84	480	286.79	0.674	650	274.59	1.37
136	532	288.91	0.84	480	286.79	0.674	650	274.59	1.37
136.5	532	288.91	0.84	480	286.79	0.674	650	274.59	1.37
137	532	288.91	0.84	480	286.79	0.674	650	274.59	1.37
137.5	532	288.91	0.84	480	286.79	0.674	650	274.59	1.37
138	532	288.91	0.84	480	286.79	0.674	650	274.59	1.37
138.5	532	288.91	0.84	480	286.79	0.674	650	274.59	1.37
139	532	288.91	0.84	480	286.79	0.674	650	274.59	1.37
139.5	532	288.91	0.84	480	286.79	0.674	650	274.59	1.37
140	532	288.91	0.84	480	286.79	0.674	650	274.59	1.37
140.5	532	288.91	0.84	480	286.79	0.674	650	274.59	1.37

141	532	288.91	0.84	480	286.79	0.674	650	274.59	1.37
141.5	532	288.91	0.84	480	286.79	0.674	650	274.59	1.37
142	532	288.91	0.84	480	286.79	0.674	650	274.59	1.37
142.5	532	288.91	0.84	480	286.79	0.674	650	274.59	1.37
143	532	288.91	0.84	480	286.79	0.674	650	274.59	1.37
143.5	532	288.91	0.84	480	286.79	0.674	650	274.59	1.37
144	532	288.91	0.84	480	286.79	0.674	650	274.59	1.37
144.5	532	288.91	0.84	480	286.79	0.674	650	274.59	1.37
145	532	288.91	0.84	480	286.79	0.674	650	274.59	1.37
145.5	532	288.91	0.84	480	286.79	0.674	650	274.59	1.37
146	532	288.91	0.84	480	286.79	0.674	650	274.59	1.37
146.5	532	288.91	0.84	480	286.79	0.674	650	274.59	1.37
147	532	288.91	0.84	480	286.79	0.674	650	274.59	1.37
147.5	532	288.91	0.84	480	286.79	0.674	650	274.59	1.37
148	532	288.91	0.84	480	286.79	0.674	650	274.59	1.37
148.5	532	288.91	0.84	480	286.79	0.674	650	274.59	1.37
149	532	288.91	0.84	480	286.79	0.674	650	274.59	1.37
149.5	532	288.91	0.84	480	286.79	0.674	650	274.59	1.37
150	532	288.91	0.84	480	286.79	0.674	650	274.59	1.37
150.5	532	288.91	0.84	480	286.79	0.674	650	274.59	1.37
151	532	288.91	0.84	480	286.79	0.674	650	274.59	1.37
151.5	532	288.91	0.84	480	286.79	0.674	650	274.59	1.37
152	532	288.91	0.84	480	286.79	0.674	650	274.59	1.37
152.5	532	288.91	0.84	480	286.79	0.674	650	274.59	1.37
153	532	288.91	0.84	480	286.79	0.674	650	274.59	1.37
153.5	532	288.91	0.84	480	286.79	0.674	650	274.59	1.37
154	532	288.91	0.84	480	286.79	0.674	650	274.59	1.37
154.5	532	288.91	0.84	480	286.79	0.674	650	274.59	1.37
155	532	288.91	0.84	480	286.79	0.674	650	274.59	1.37
155.5	532	288.91	0.84	480	286.79	0.674	650	274.59	1.37
156	532	288.91	0.84	480	286.79	0.674	650	274.59	1.37
156.5	532	288.91	0.84	480	286.79	0.674	650	274.59	1.37
157	532	288.91	0.84	480	286.79	0.674	650	274.59	1.37
157.5	532	288.91	0.84	480	286.79	0.674	650	274.59	1.37
158	532	288.91	0.84	480	286.79	0.674	650	274.59	1.37
158.5	532	288.91	0.84	480	286.79	0.674	650	274.59	1.37

159	532	288.91	0.84	480	286.79	0.674	650	274.59	1.37
159.5	532	288.91	0.84	480	286.79	0.674	650	274.59	1.37
160	532	288.91	0.84	480	286.79	0.674	650	274.59	1.37
160.5	532	288.91	0.84	480	286.79	0.674	650	274.59	1.37
161	532	288.91	0.84	480	286.79	0.674	650	274.59	1.37
161.5	532	288.91	0.84	480	286.79	0.674	650	274.59	1.37
162	532	288.91	0.84	480	286.79	0.674	650	274.59	1.37
162.5	532	288.91	0.84	480	286.79	0.674	660	274.59	1.40
163	532	288.91	0.84	480	286.79	0.674	660	274.59	1.40
163.5	532	288.91	0.84	480	286.79	0.674	660	274.59	1.40
164	532	288.91	0.84	480	286.79	0.674	660	274.59	1.40
164.5	532	288.91	0.84	480	286.79	0.674	660	274.59	1.40
165	532	288.91	0.84	480	286.79	0.674	660	274.59	1.40
165.5	532	288.91	0.84	480	286.79	0.674	660	274.59	1.40
166	532	288.91	0.84	480	286.79	0.674	660	274.59	1.40
166.5	532	288.91	0.84	480	286.79	0.674	660	274.59	1.40
167	530	288.91	0.83	480	286.79	0.674	660	274.59	1.40
167.5	531	288.91	0.84	480	286.79	0.674	660	274.59	1.40
168	531	288.91	0.84	480	286.79	0.674	660	274.59	1.40
168.5	531	288.91	0.84	480	286.79	0.674	660	274.59	1.40
169	531	288.91	0.84	480	286.79	0.674	660	274.59	1.40
169.5	531	288.91	0.84	480	286.79	0.674	660	274.59	1.40
170	531	288.91	0.84	480	286.79	0.674	660	274.59	1.40
170.5	531	288.91	0.84	480	286.79	0.674	660	274.59	1.40
171	531	288.91	0.84	480	286.79	0.674	660	274.59	1.40
171.5	531	288.91	0.84	480	286.79	0.674	660	274.59	1.40
172	531	288.91	0.84	480	286.79	0.674	660	274.59	1.40
172.5	531	288.91	0.84	480	286.79	0.674	660	274.59	1.40
173	531	288.91	0.84	480	286.79	0.674	660	274.59	1.40
173.5	531	288.91	0.84	480	286.79	0.674	660	274.59	1.40
174	531	288.91	0.84	480	286.79	0.674	660	274.59	1.40
174.5	531	288.91	0.84	480	286.79	0.674	660	274.59	1.40
175	531	288.91	0.84	480	286.79	0.674	660	274.59	1.40
175.5	531	288.91	0.84	480	286.79	0.674	660	274.59	1.40
176	531	288.91	0.84	480	286.79	0.674	660	274.59	1.40
176.5	531	288.91	0.84	480	286.79	0.674	660	274.59	1.40

177	531	288.91	0.84	480	286.79	0.674	660	274.59	1.40
177.5	531	288.91	0.84	480	286.79	0.674	660	274.59	1.40
178	531	288.91	0.84	480	286.79	0.674	660	274.59	1.40
178.5	531	288.91	0.84	480	286.79	0.674	660	274.59	1.40
179	531	288.91	0.84	480	286.79	0.674	660	274.59	1.40
179.5	531	288.91	0.84	480	286.79	0.674	660	274.59	1.40
180	531	288.91	0.84	480	286.79	0.674	660	274.59	1.40
180.5	531	288.91	0.84	480	286.79	0.674	660	274.59	1.40
181	531	288.91	0.84	480	286.79	0.674	660	274.59	1.40
181.5	531	288.91	0.84	480	286.79	0.674	660	274.59	1.40
182	531	288.91	0.84	480	286.79	0.674	660	274.59	1.40
182.5	531	288.91	0.84	480	286.79	0.674	660	274.59	1.40
183	531	288.91	0.84	480	286.79	0.674	660	274.59	1.40
183.5	531	288.91	0.84	480	286.79	0.674	660	274.59	1.40
184	531	288.91	0.84	480	286.79	0.674	660	274.59	1.40
184.5	531	288.91	0.84	480	286.79	0.674	670	274.59	1.44
185	531	288.91	0.84	480	286.79	0.674	670	274.59	1.44
185.5	531	288.91	0.84	480	286.79	0.674	670	274.59	1.44
186	531	288.91	0.84	480	286.79	0.674	670	274.59	1.44
186.5	531	288.91	0.84	480	286.79	0.674	670	274.59	1.44
187	531	288.91	0.84	480	286.79	0.674	670	274.59	1.44
187.5	531	288.91	0.84	480	286.79	0.674	670	274.59	1.44
188	531	288.91	0.84	480	286.79	0.674	670	274.59	1.44
188.5	531	288.91	0.84	480	286.79	0.674	670	274.59	1.44
189	531	288.91	0.84	480	286.79	0.674	670	274.59	1.44
189.5	531	288.91	0.84	480	286.79	0.674	670	274.59	1.44
190	531	288.91	0.84	480	286.79	0.674	660	274.59	1.40
190.5	531	288.91	0.84	480	286.79	0.674	660	274.59	1.40
191	531	288.91	0.84	480	286.79	0.674	660	274.59	1.40
191.5	531	288.91	0.84	480	286.79	0.674	660	274.59	1.40
192	531	288.91	0.84	480	286.79	0.674	660	274.59	1.40
192.5	531	288.91	0.84	480	286.79	0.674	660	274.59	1.40
193	531	288.91	0.84	480	286.79	0.674	660	274.59	1.40
193.5	531	288.91	0.84	480	286.79	0.674	660	274.59	1.40
194	531	288.91	0.84	480	286.79	0.674	660	274.59	1.40
194.5	531	288.91	0.84	480	286.79	0.674	660	274.59	1.40

195	531	288.91	0.84	480	286.79	0.674	660	274.59	1.40
195.5	531	288.91	0.84	480	286.79	0.674	660	274.59	1.40
196	531	288.91	0.84	480	286.79	0.674	660	274.59	1.40
196.5	531	288.91	0.84	480	286.79	0.674	650	274.59	1.37
197	531	288.91	0.84	480	286.79	0.674	650	274.59	1.37
197.5	531	288.91	0.84	480	286.79	0.674	650	274.59	1.37
198	531	288.91	0.84	480	286.79	0.674	650	274.59	1.37
198.5	531	288.91	0.84	480	286.79	0.674	650	274.59	1.37
199	531	288.91	0.84	480	286.79	0.674	650	274.59	1.37
199.5	531	288.91	0.84	480	286.79	0.674	650	274.59	1.37
200	531	288.91	0.84	480	286.79	0.674	650	274.59	1.37
200.5	531	288.91	0.84	480	286.79	0.674	650	274.59	1.37
201	531	288.91	0.84	480	286.79	0.674	650	274.59	1.37
201.5	531	288.91	0.84	480	286.79	0.674	650	274.59	1.37
202	531	288.91	0.84	480	286.79	0.674	650	274.59	1.37
202.5	531	288.91	0.84	480	286.79	0.674	650	274.59	1.37
203	531	288.91	0.84	480	286.79	0.674	650	274.59	1.37
203.5	525	288.91	0.82	480	286.79	0.674	650	274.59	1.37
204	525	288.91	0.82	480	286.79	0.674	650	274.59	1.37
204.5	525	288.91	0.82	480	286.79	0.674	650	274.59	1.37
205	525	288.91	0.82	480	286.79	0.674	650	274.59	1.37
205.5	525	288.91	0.82	480	286.79	0.674	650	274.59	1.37
206	525	288.91	0.82	480	286.79	0.674	650	274.59	1.37
206.5	525	288.91	0.82	480	286.79	0.674	650	274.59	1.37
207	525	288.91	0.82	480	286.79	0.674	650	274.59	1.37
207.5	525	288.91	0.82	480	286.79	0.674	650	274.59	1.37
208	525	288.91	0.82	480	286.79	0.674	650	274.59	1.37
208.5	525	288.91	0.82	480	286.79	0.674	650	274.59	1.37
209	525	288.91	0.82	480	286.79	0.674	650	274.59	1.37
209.5	525	288.91	0.82	480	286.79	0.674	650	274.59	1.37
210	525	288.91	0.82	480	286.79	0.674	650	274.59	1.37
210.5	525	288.91	0.82	480	286.79	0.674	650	274.59	1.37
211	525	288.91	0.82	480	286.79	0.674	650	274.59	1.37
211.5	525	288.91	0.82	480	286.79	0.674	650	274.59	1.37
212	525	288.91	0.82	480	286.79	0.674	650	274.59	1.37
212.5	525	288.91	0.81	480	286.79	0.674	650	274.59	1.37

213	525	288.91	0.82	480	286.79	0.674	650	274.59	1.37
213.5	525	288.91	0.82	480	286.79	0.674	650	274.59	1.37
214	525	288.91	0.82	480	286.79	0.674	650	274.59	1.37
214.5	525	288.91	0.82	480	286.79	0.674	650	274.59	1.37
215	525	288.91	0.82	480	286.79	0.674	650	274.59	1.37
215.5	525	288.91	0.82	480	286.79	0.674	650	274.59	1.37
216	525	288.91	0.82	480	286.79	0.674	650	274.59	1.37
216.5	525	288.91	0.82	480	286.79	0.674	650	274.59	1.37
217	525	288.91	0.82	480	286.79	0.674	650	274.59	1.37
217.5	525	288.91	0.82	480	286.79	0.674	650	274.59	1.37
218	525	288.91	0.82	480	286.79	0.674	650	274.59	1.37
218.5	525	288.91	0.82	480	286.79	0.674	650	274.59	1.37
219	525	288.91	0.82	480	286.79	0.674	650	274.59	1.37
219.5	525	288.91	0.82	480	286.79	0.674	650	274.59	1.37
220	525	288.91	0.82	480	286.79	0.674	650	274.59	1.37
220.5	525	288.91	0.82	480	286.79	0.674	650	274.59	1.37
221	525	288.91	0.82	480	286.79	0.674	650	274.59	1.37
221.5	525	288.91	0.82	480	286.79	0.674	650	274.59	1.37
222	525	288.91	0.82	480	286.79	0.674	650	274.59	1.37
222.5	525	288.91	0.82	480	286.79	0.674	650	274.59	1.37
223	525	288.91	0.82	480	286.79	0.674	650	274.59	1.37
223.5	525	288.91	0.82	480	286.79	0.674	650	274.59	1.37
224	525	288.91	0.82	480	286.79	0.674	650	274.59	1.37
224.5	525	288.91	0.82	480	286.79	0.674	650	274.59	1.37
225	525	288.91	0.82	480	286.79	0.674	650	274.59	1.37
225.5	525	288.91	0.82	480	286.79	0.674	650	274.59	1.37
226	525	288.91	0.82	480	286.79	0.674	650	274.59	1.37
226.5	525	288.91	0.82	480	286.79	0.674	650	274.59	1.37
227	525	288.91	0.82	480	286.79	0.674	650	274.59	1.37
227.5	525	288.91	0.82	480	286.79	0.674	650	274.59	1.37
228	525	288.91	0.82	480	286.79	0.674	650	274.59	1.37
228.5	525	288.91	0.82	480	286.79	0.674	650	274.59	1.37
229	525	288.91	0.82	480	286.79	0.674	650	274.59	1.37
229.5	520	288.91	0.80	480	286.79	0.674	650	274.59	1.37
230	520	288.91	0.80	480	286.79	0.674	650	274.59	1.37
230.5	520	288.91	0.80	480	286.79	0.674	650	274.59	1.37

231	520	288.91	0.80	480	286.79	0.674	650	274.59	1.37
231.5	520	288.91	0.80	480	286.79	0.674	650	274.59	1.37
232	520	288.91	0.80	480	286.79	0.674	650	274.59	1.37
232.5	520	288.91	0.80	480	286.79	0.674	650	274.59	1.37
233	520	288.91	0.80	480	286.79	0.674	650	274.59	1.37
233.5	520	288.91	0.80	480	286.79	0.674	650	274.59	1.37
234	520	288.91	0.80	480	286.79	0.674	650	274.59	1.37
234.5	520	288.91	0.80	480	286.79	0.674	650	274.59	1.37
235	520	288.91	0.80	480	286.79	0.674	650	274.59	1.37
235.5	520	288.91	0.80	480	286.79	0.674	650	274.59	1.37
236	520	288.91	0.80	480	286.79	0.674	650	274.59	1.37
236.5	520	288.91	0.80	480	286.79	0.674	650	274.59	1.37
237	520	288.91	0.80	480	286.79	0.674	650	274.59	1.37
237.5	520	288.91	0.80	480	286.79	0.674	650	274.59	1.37
238	520	288.91	0.80	480	286.79	0.674	650	274.59	1.37
238.5	520	288.91	0.80	480	286.79	0.674	650	274.59	1.37
239	520	288.91	0.80	480	286.79	0.674	650	274.59	1.37
239.5	520	288.91	0.80	480	286.79	0.674	650	274.59	1.37
240	520	288.91	0.80	480	286.79	0.674	650	274.59	1.37
240.5	520	288.91	0.80	480	286.79	0.674	650	274.59	1.37
241	520	288.91	0.80	480	286.79	0.674	650	274.59	1.37
241.5	520	288.91	0.80	480	286.79	0.674	650	274.59	1.37
242	520	288.91	0.80	480	286.79	0.674	650	274.59	1.37
242.5	520	288.91	0.80	480	286.79	0.674	650	274.59	1.37
243	520	288.91	0.80	480	286.79	0.674	650	274.59	1.37
243.5	520	288.91	0.80	480	286.79	0.674	650	274.59	1.37
244	520	288.91	0.80	480	286.79	0.674	650	274.59	1.37
244.5	520	288.91	0.80	480	286.79	0.674	650	274.59	1.37
245	520	288.91	0.80	480	286.79	0.674	650	274.59	1.37
245.5	520	288.91	0.80	480	286.79	0.674	650	274.59	1.37
246	520	288.91	0.80	480	286.79	0.674	650	274.59	1.37
246.5	520	288.91	0.80	480	286.79	0.674	650	274.59	1.37
247	520	288.91	0.80	480	286.79	0.674	650	274.59	1.37
247.5	520	288.91	0.80	480	286.79	0.674	650	274.59	1.37
248	520	288.91	0.80	480	286.79	0.674	650	274.59	1.37
248.5	520	288.91	0.80	480	286.79	0.674	650	274.59	1.37

249	520	288.91	0.80	480	286.79	0.674	650	274.59	1.37
249.5	520	288.91	0.80	480	286.79	0.674	650	274.59	1.37
250	520	288.91	0.80	480	286.79	0.674	650	274.59	1.37
250.5	520	288.91	0.80	480	286.79	0.674	650	274.59	1.37
251	520	288.91	0.80	480	286.79	0.674	650	274.59	1.37
251.5	520	288.91	0.80	480	286.79	0.674	650	274.59	1.37
252	520	288.91	0.80	480	286.79	0.674	650	274.59	1.37
252.5	520	288.91	0.80	480	286.79	0.674	650	274.59	1.37
253	520	288.91	0.80	480	286.79	0.674	650	274.59	1.37
253.5	520	288.91	0.80	480	286.79	0.674	650	274.59	1.37
254	520	288.91	0.80	480	286.79	0.674	650	274.59	1.37
254.5	520	288.91	0.80	480	286.79	0.674	650	274.59	1.37
255	520	288.91	0.80	480	286.79	0.674	650	274.59	1.37
255.5	520	288.91	0.80	480	286.79	0.674	650	274.59	1.37
256	520	288.91	0.80	480	286.79	0.674	650	274.59	1.37
256.5	520	288.91	0.80	480	286.79	0.674	650	274.59	1.37
257	520	288.91	0.80	480	286.79	0.674	650	274.59	1.37
257.5	520	288.91	0.80	480	286.79	0.674	650	274.59	1.37
258	520	288.91	0.80	480	286.79	0.674	650	274.59	1.37
258.5	520	288.91	0.80	480	286.79	0.674	650	274.59	1.37
259	520	288.91	0.80	480	286.79	0.674	650	274.59	1.37
259.5	520	288.91	0.80	480	286.79	0.674	650	274.59	1.37
260	520	288.91	0.80	480	286.79	0.674	650	274.59	1.37
260.5	520	288.91	0.80	480	286.79	0.674	650	274.59	1.37
261	520	288.91	0.80	480	286.79	0.674	650	274.59	1.37
261.5	520	288.91	0.80	480	286.79	0.674	650	274.59	1.37
262	520	288.91	0.80	480	286.79	0.674	650	274.59	1.37
262.5	520	288.91	0.80	480	286.79	0.674	650	274.59	1.37
263	520	288.91	0.80	480	286.79	0.674	650	274.59	1.37
263.5	520	288.91	0.80	480	286.79	0.674	650	274.59	1.37
264	520	288.91	0.80	480	286.79	0.674	650	274.59	1.37
264.5	520	288.91	0.80	480	286.79	0.674	650	274.59	1.37
265	520	288.91	0.80	480	286.79	0.674	650	274.59	1.37
265.5	520	288.91	0.80	480	286.79	0.674	650	274.59	1.37
266	520	288.91	0.80	480	286.79	0.674	650	274.59	1.37
266.5	520	288.91	0.80	480	286.79	0.674	650	274.59	1.37

267	520	288.91	0.80	480	286.79	0.674	650	274.59	1.37
267.5	520	288.91	0.80	480	286.79	0.674	650	274.59	1.37
268	520	288.91	0.80	480	286.79	0.674	650	274.59	1.37
268.5	520	288.91	0.80	480	286.79	0.674	650	274.59	1.37
269	520	288.91	0.80	480	286.79	0.674	650	274.59	1.37
269.5	520	288.91	0.80	480	286.79	0.674	650	274.59	1.37
270	520	288.91	0.80	480	286.79	0.674	650	274.59	1.37
270.5	520	288.91	0.80	480	286.79	0.674	650	274.59	1.37
271	520	288.91	0.80	480	286.79	0.674	650	274.59	1.37
271.5	520	288.91	0.80	480	286.79	0.674	650	274.59	1.37
272	520	288.91	0.80	480	286.79	0.674	650	274.59	1.37
272.5	520	288.91	0.80	480	286.79	0.674	650	274.59	1.37
273	520	288.91	0.80	480	286.79	0.674	650	274.59	1.37
273.5	520	288.91	0.80	480	286.79	0.674	650	274.59	1.37
274	520	288.91	0.80	480	286.79	0.674	650	274.59	1.37
274.5	520	288.91	0.80	480	286.79	0.674	650	274.59	1.37
275	520	288.91	0.80	480	286.79	0.674	650	274.59	1.37
275.5	520	288.91	0.80	480	286.79	0.674	650	274.59	1.37
276	520	288.91	0.80	480	286.79	0.674	650	274.59	1.37
276.5	520	288.91	0.80	480	286.79	0.674	650	274.59	1.37
277	520	288.91	0.80	480	286.79	0.674	650	274.59	1.37
277.5	520	288.91	0.80	480	286.79	0.674	650	274.59	1.37
278	520	288.91	0.80	480	286.79	0.674	650	274.59	1.37
278.5	520	288.91	0.80	480	286.79	0.674	650	274.59	1.37
279	520	288.91	0.80	480	286.79	0.674	650	274.59	1.37
279.5	520	288.91	0.80	480	286.79	0.674	650	274.59	1.37
280	520	288.91	0.80	480	286.79	0.674	650	274.59	1.37
280.5	520	288.91	0.80	480	286.79	0.674	650	274.59	1.37
281	520	288.91	0.80	480	286.79	0.674	650	274.59	1.37
281.5	520	288.91	0.80	480	286.79	0.674	650	274.59	1.37
282	520	288.91	0.80	480	286.79	0.674	650	274.59	1.37
282.5	520	288.91	0.80	480	286.79	0.674	650	274.59	1.37
283	520	288.91	0.80	480	286.79	0.674	650	274.59	1.37
283.5	520	288.91	0.80	480	286.79	0.674	650	274.59	1.37
284	520	288.91	0.80	480	286.79	0.674	650	274.59	1.37
284.5	520	288.91	0.80	480	286.79	0.674	650	274.59	1.37

285	520	288.91	0.80	480	286.79	0.674	650	274.59	1.37
285.5	520	288.91	0.80	480	286.79	0.674	650	274.59	1.37
286	520	288.91	0.80	480	286.79	0.674	650	274.59	1.37
286.5	520	288.91	0.80	480	286.79	0.674	650	274.59	1.37
287	520	288.91	0.80	480	286.79	0.674	650	274.59	1.37
287.5	520	288.91	0.80	480	286.79	0.674	650	274.59	1.37
288	520	288.91	0.80	480	286.79	0.674	650	274.59	1.37
288.5	520	288.91	0.80	480	286.79	0.674	650	274.59	1.37
289	520	288.91	0.80	480	286.79	0.674	650	274.59	1.37
289.5	520	288.91	0.80	480	286.79	0.674	650	274.59	1.37

APPENDIX B

DATA COLLECTED FROM LITERATURE

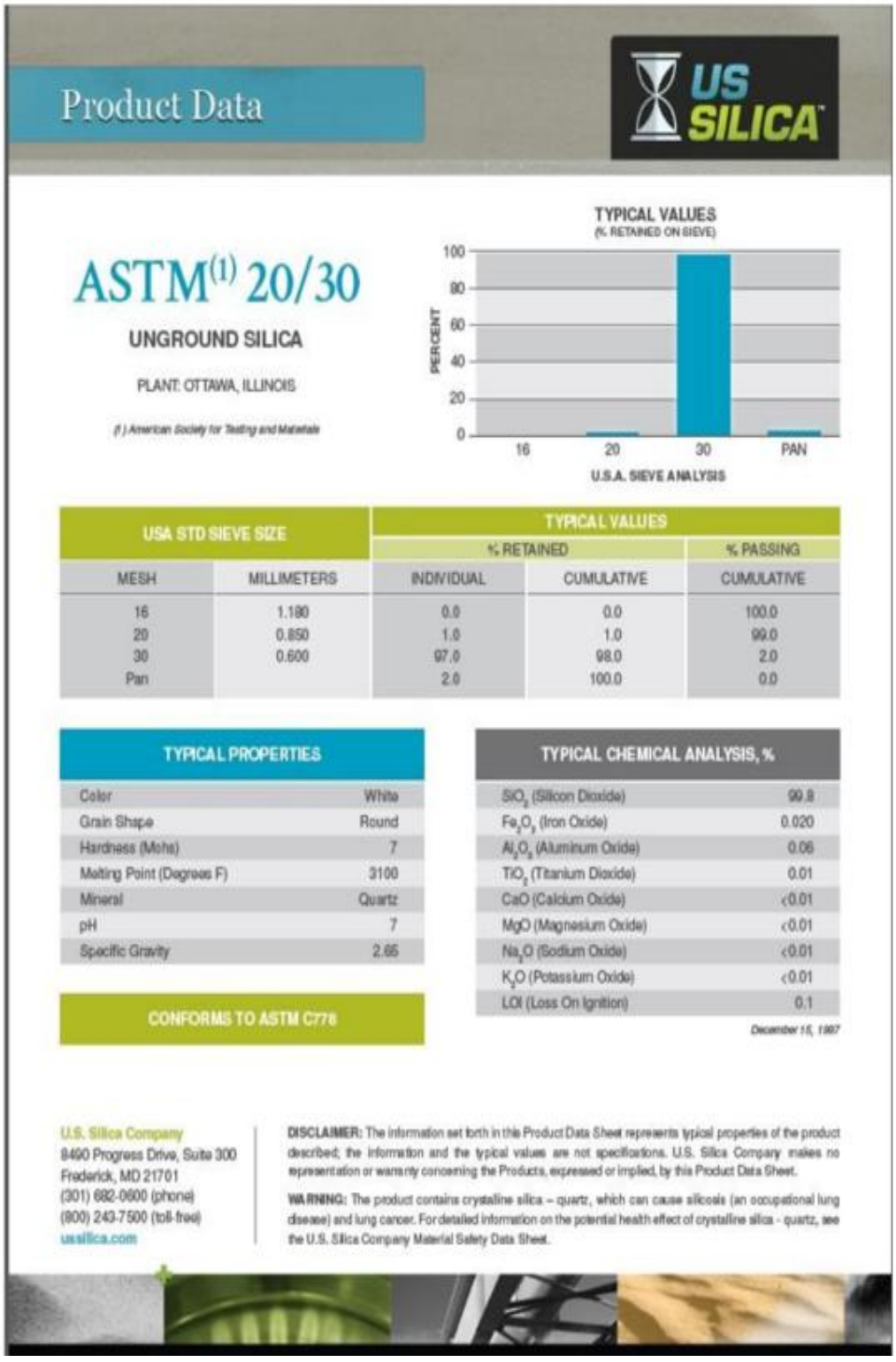

Product Data

US SILICA

ASTM(1) 20/30

UNGROUND SILICA

PLANT: OTTAWA, ILLINOIS

(1) American Society for Testing and Materials

USA STD SIEVE SIZE		TYPICAL VALUES		
		% RETAINED		% PASSING
MESH	MILLIMETERS	INDIVIDUAL	CUMULATIVE	CUMULATIVE
16	1.180	0.0	0.0	100.0
20	0.850	1.0	1.0	99.0
30	0.600	97.0	98.0	2.0
Pan		2.0	100.0	0.0

TYPICAL PROPERTIES	
Color	White
Grain Shape	Round
Hardness (Mohs)	7
Melting Point (Degrees F)	3100
Mineral	Quartz
pH	7
Specific Gravity	2.65

CONFORMS TO ASTM C778

TYPICAL CHEMICAL ANALYSIS, %	
SiO_2 (Silicon Dioxide)	99.8
Fe_2O_3 (Iron Oxide)	0.020
Al_2O_3 (Aluminum Oxide)	0.06
TiO_2 (Titanium Dioxide)	0.01
CaO (Calcium Oxide)	<0.01
MgO (Magnesium Oxide)	<0.01
Na_2O (Sodium Oxide)	<0.01
K_2O (Potassium Oxide)	<0.01
LOI (Loss On Ignition)	0.1

December 15, 1997

U.S. Silica Company
8490 Progress Drive, Suite 300
Frederick, MD 21701
(301) 682-0600 (phone)
(800) 243-7500 (toll-free)
ussilica.com

DISCLAIMER: The information set forth in this Product Data Sheet represents typical properties of the product described; the information and the typical values are not specifications. U.S. Silica Company makes no representation or warranty concerning the Products, expressed or implied, by this Product Data Sheet.

WARNING: The product contains crystalline silica – quartz, which can cause silicosis (an occupational lung disease) and lung cancer. For detailed information on the potential health effect of crystalline silica - quartz, see the U.S. Silica Company Material Safety Data Sheet.

Figure 24 :Product Data for Ottawa 20-30 sand (Guiterraz, 2013)

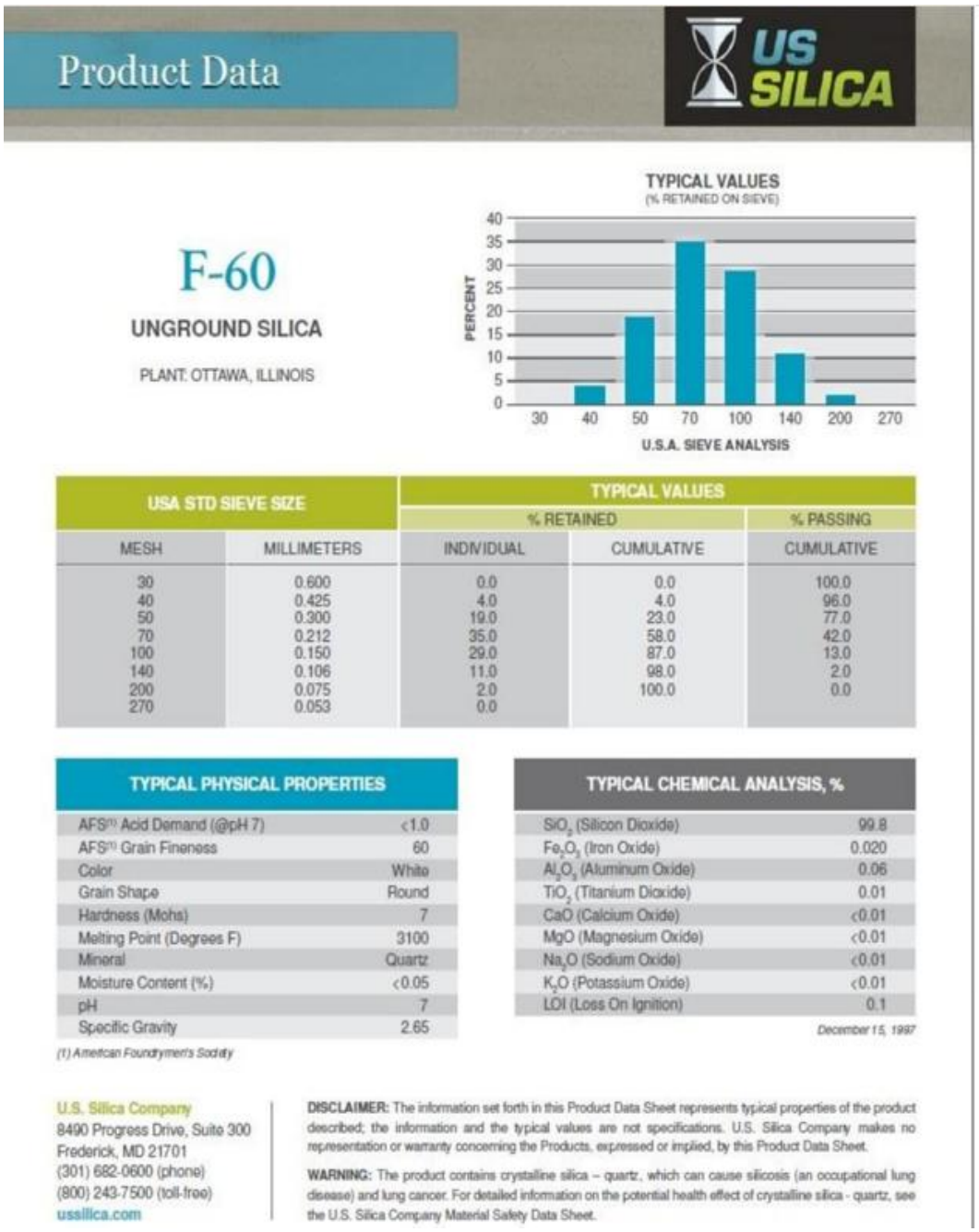

Product Data

US SILICA

F-60

UNGROUND SILICA

PLANT: OTTAWA, ILLINOIS

USA STD SIEVE SIZE		TYPICAL VALUES		
		% RETAINED		% PASSING
MESH	MILLIMETERS	INDIVIDUAL	CUMULATIVE	CUMULATIVE
30	0.600	0.0	0.0	100.0
40	0.425	4.0	4.0	96.0
50	0.300	19.0	23.0	77.0
70	0.212	35.0	58.0	42.0
100	0.150	29.0	87.0	13.0
140	0.106	11.0	98.0	2.0
200	0.075	2.0	100.0	0.0
270	0.053	0.0		

TYPICAL PHYSICAL PROPERTIES	
AFS[1] Acid Demand (@pH 7)	<1.0
AFS[1] Grain Fineness	60
Color	White
Grain Shape	Round
Hardness (Mohs)	7
Melting Point (Degrees F)	3100
Mineral	Quartz
Moisture Content (%)	<0.05
pH	7
Specific Gravity	2.65

(1) American Foundrymen's Society

TYPICAL CHEMICAL ANALYSIS, %	
SiO_2 (Silicon Dioxide)	99.8
Fe_2O_3 (Iron Oxide)	0.020
Al_2O_3 (Aluminum Oxide)	0.06
TiO_2 (Titanium Dioxide)	0.01
CaO (Calcium Oxide)	<0.01
MgO (Magnesium Oxide)	<0.01
Na_2O (Sodium Oxide)	<0.01
K_2O (Potassium Oxide)	<0.01
LOI (Loss On Ignition)	0.1

December 15, 1997

U.S. Silica Company
8490 Progress Drive, Suite 300
Frederick, MD 21701
(301) 682-0600 (phone)
(800) 243-7500 (toll-free)
ussilica.com

Figure 25 : Product Data for F-60 sand (Guiterraz, 2013)